42nd AIAA/ASME/SAE/ASEE Joint Propulsion Conference & Exhibit
9 - 12 July 2006, Sacramento, California

AIAA 2006-4453

S-Shaped Inlet Design Optimization Using the Adjoint Equation Method

Zhengke Zhang[*,†]
National Key Laboratory of Aerodynamic Design and Research, Northwestern Poly-technical University, Xi'an 710072, P. R. China

Kai-Yew Lum[‡]
Temasek Laboratories, National University of Singapore, 5 Sports Drive 2, Singapore 117508

This paper presents an application of the adjoint equation method, a well-established method for aerodynamic shape optimization in external flow, to the internal-flow problem of engine inlet design. A serpentine shaped duct with prescribed entrance and exit geometries is considered, where the design objective is to optimize the curvature and cross-sections of the duct in order to reduce flow distortion at the exit. In an indirect formulation of the problem, the wall pressure drag is chosen as objective function, under which the adjoint method can be formulated. Inviscid flow is considered, with the Euler equation and its adjoint as governing equations. The results show that this leads in return to an improved uniformity of the exit-face total pressure, albeit with slight loss in the average total pressure.

I. Introduction

FOR supersonic aircraft, the inlet is used as a velocity decelerator and pre-compressing unit other than the compressor[1]. For inlets mounted along the center-line of a fuselage, there exists a center-body (spike) which is used to compress the air[2]. For side-mounted inlet, no center-body exists[3], the air is compressed by a ramp or several consecutive ramps[4-6]. In general, adverse pressure gradient exists in the axial direction, thus the boundary layer is susceptible to separation. Moreover, in supersonic flow shocks are formed due to compression, or when the flow is deflected, which may also induce separation. In addition to viscosity, these flow phenomena lead to energy loss characterized by total-pressure loss[1,7]. Shock/boundary layer interaction in inlets may also cause shock oscillation, leading to engine surge or buzz[8-10].

In military applications, serpentine shaped ducts are often used as inlets to prevent radar scattering by the engine fan blades, which introduces additional problems besides the existing problems in conventional inlets. In particular, the curvature of the s-shaped duct may cause a cross swirl (cross-section rotation, generally with two counter-rotating vortices) which will be further aggravated by maneuver. Cross swirl as well as streamwise boundary layer separation increase the flow field distortion at the compressor face, characterized by loss as well as non-uniformity of the total pressure. This is one of the leading causes of excessive vibration of the fan blades and high-cycle fatigue damage, decreased efficiency, and restricts the engine's surge and stall limits.[11-15]

In view of the above, optimal design of supersonic s-shaped inlets is of practical interest. For example, Gaiddon and Knight[3] claimed that evolutionary strategies are better than gradient-based method in terms of performance improvement. On the other hand, the adjoint equation method has been successfully used in 2-d airfoil and 3-d wing shape design optimization[16-19]. The advantage of the method is that only one flow field solution and one adjoint equation solution are needed at each design cycle in order to compute the gradient, making it more efficient than methods based on finite differencing. Obviously, like all gradient-based methods, the adjoint method is less time-consuming than genetic algorithms, but allows only local optima to be found.

In this paper we shall explore the adjoint method for s-shaped inlet design optimization. Given fixed entrance and exit diameters and a vertical offset between the locations of the entrance and exit, the objective is to optimize the centerline-curvature and cross-section diameters of the duct. Following the comments in the preceding paragraphs, a direct formulation would be to minimize both the total-pressure loss and non-uniformity at the exit

[*] Professor.
[†] Research Scientist (Sept. 2001-Sept. 2005), Temasek Laboratories, National University of Singapore
[‡] Principal Research Scientist.

face; however an adjoint formulation with these quantities as cost functions is inextricable. Instead, we shall adopt an indirect approach consisting in minimizing the surface drag along the wall of the inlet, based on the consideration that total-pressure loss and non-uniformity result from irreversible factors such as shock waves and friction, which will be reflected in the surface drag. With the latter as cost function, an adjoint formulation can be derived. We shall consider only inviscid flow in this study using the Euler equations as governing equation; thus, only the effects of shock will be accounted and not those of skin friction. The results presented in later section will show that this approach effectively leads to improvement in the uniformity of exit-face total pressure, but does not prevent further loss in total pressure.

II. Problem Description

In this study, we model the inlet as an s-shaped duct with circular cross-sections, oriented length-wise in the x direction, and symmetrical about the *x*-*z* plane. For the design problem, we assume fixed values for the entrance diameter r_1, exit diameter r_2, and distance L between the entrance and exit along the *x*-axis. Moreover, we also assume that the vertical offset *s* between the centers of entrance and exit is fixed. (See Fig. 1). These assumptions are reasonable as those dimensions are often dictated by fuselage configuration. The shape of the duct is then completely defined by its centerline, and the cross-section radius distribution $r(x)$ along the *x*-axis. (In later sections, we shall alternatively use indicial notations x_1, x_2, x_3 to stand for *x, y, z*, respectively.)

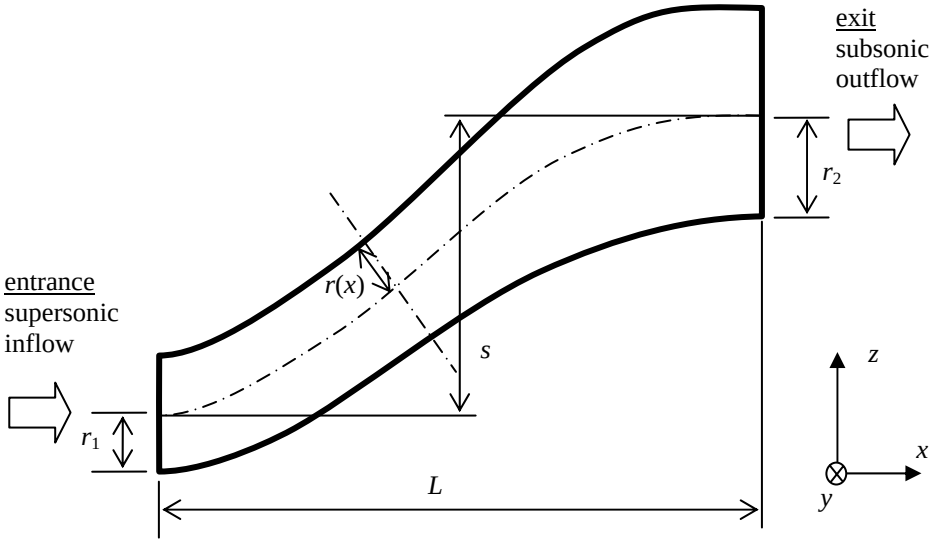

Fig. 1 Definition of an inlet shape (sectional view in symmetry plane)

We consider the problem where the inflow is supersonic at zero angle of attack relative to the *x*-axis, and where the outflow is subsonic. The design problem consists in varying the centerline shape and the cross-section radius distribution in order to minimize an aerodynamic cost function to be defined later. In order to ensure that the optimization produces reasonable shapes, we allow the centerline and radius distribution to vary about a baseline design. First, we shall define the *z* coordinates of the baseline centerline to be the following analytical function of *x*:

$$z_{baseline}(x) = s\left[(n+1)\left(\frac{x}{L}\right)^n - n\left(\frac{x}{L}\right)^{n+1}\right] \tag{2.1a}$$

This function has the property that both ends ($x/L = 0,\ \ x/L = 1$) are tangential to the *x*-axis. The baseline radius distribution $r_{baseline}(x)$ may take a similar form:

$$r_{baseline}(x) = r_1 + (r_2 - r_1)\left[(n+1)\left(\frac{x}{L}\right)^n - n\left(\frac{x}{L}\right)^{n+1}\right] \quad (2.1b)$$

where in typical applications, $r_1 < r_2$, i.e., the exit is usually larger than the entrance. The baseline shape is thus completely determined. The basic function $f(x) = (n+1)x^n - nx^{n+1}$ $(0 \le x \le 1)$ with different powers is plotted in Fig. 2 for comparison.

Now, we consider the problem space to be the set of shapes defined as a summation of the baseline shape and a perturbation that consists of a linear combination of Hicks-Henne basis functions[20,21]; such shape functions have been widely used in airfoil design optimization. In other words, we consider centerline functions and radius distribution functions of the parametric form:

$$z(x) = z_{baseline}(x) + \sum_{k=1}^{K} \alpha_k h_k(x) \quad (2.2a)$$

$$r(x) = r_{baseline}(x) + \sum_{k=1}^{K} \alpha_{K+k} h_k(x) \quad (2.2b)$$

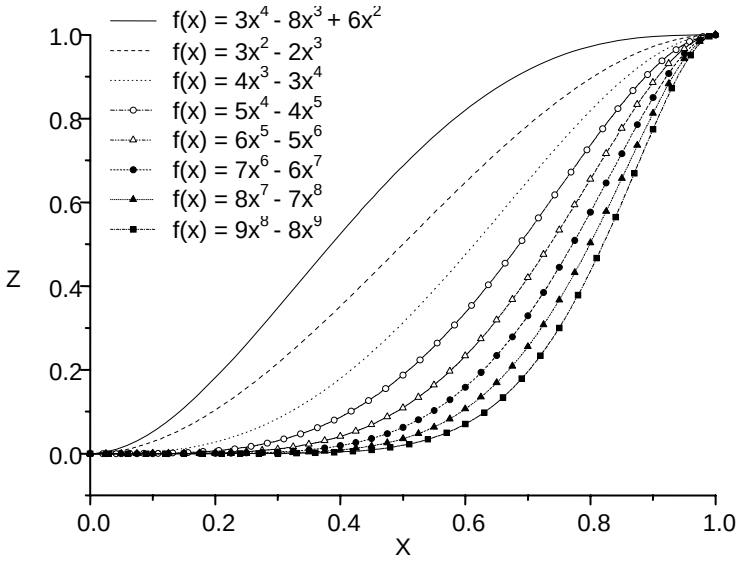

Fig. 2 Comparison of base shapes

where K is a chosen number, and α_k (k = 1, … , 2K) are the design parameters. Note that z and r are independently defined, each with K parameters, although the same Hicks-Henne basis is used. For this study, we choose a basis of 30 Hicks-Henne functions, i.e., K=30, and

$$h_k(x) = \sin^4(\pi x^{e(k)}) \quad (2.3)$$

where

$$e(k) = \log(0.5)/\log(x_k)$$

$$x_k = 0.03,0.06,0.10,0.15,0.20,0.25,0.30,0.35,0.40,0.45,0.50,0.525,0.55,0.575,$$
$$0.60,0.625,0.65,0.675,0.70,0.725,0.75,0.775,0.80,0.825,0.85,0.875,$$
$$0.90,0.925,0.95,0.975.$$

Thus, given an objective function I of the duct's aerodynamic performance, the design objective is to find the minimum $\min_{\alpha_k}\{I\}$ by varying α_k $(k = 1,...,2K)$. Obviously, the resulting shape depends on the choice of K and the basis functions h_k, which represents the problem space. A richer representation can be obtained with a larger K. Other parametric shape representations such as NURBS may also be considered.

III. Principle of the Adjoint Method

In this section, we outline the basic principle of the adjoint method[16-18]. Consider an aerodynamic shape – in this case an inlet – whose geometry S is parametrically defined as mentioned above:

$$S(x) = h_0(x) + \sum \alpha_i h_i(x) \tag{3.1}$$

Suppose I is a cost function of the flow characteristics to be minimized. Since, at given freestream and exit conditions, the aerodynamic properties of the inlet only depend on the shape, the value of I therefore depends on the coefficients α_i for given basis functions $h_i(x)$. In order words, α_i can be regarded as design variables. If the sensitivities $\partial I/\partial \alpha_i$ can be found, the resulting gradient vector may be used to determine a direction of descent in the search for an optimum shape[16], such as $\alpha^{n+1} = \alpha^n - \lambda \cdot \partial I/\partial \alpha$. In gradient-based methods using finite differencing, the sensitivities are approximated by

$$\frac{\partial I}{\partial \alpha_i} \approx \frac{I(\alpha_i + \delta\alpha_i) - I(\alpha_i)}{\delta \alpha_i}$$

and $I(\alpha_i + \delta\alpha_i)$ is obtained by recalculating the flow field for each α_i. For a total number of *N* design variables, $N+1$ flow calculations are needed for each design cycle, making such methods computationally expensive.

The adjoint method proceeds differently[16-18]. For flow inside an inlet, the aerodynamic properties are functions of the flow field variables w, and the physical location of the boundaries represented by *S*; obviously w is dependent on *S*. Thus, the cost function is also function of w and *S*:

$$I = I(w, S) \tag{3.2}$$

A change in S results in a change in the cost function I

$$\delta I = \frac{\partial I^T}{\partial w}\delta w + \frac{\partial I^T}{\partial S}\delta S$$

Using optimal control theory, the governing equations of the flow field can be introduced as a constraint between δw and δS in such a way that the final expression for the gradient does not require reevaluation of the flow field. In effect, suppose that the governing equation R, which expresses the dependence of w and S within the flow field domain Ω, can be written as

$$R(w, S) = 0$$

Then δw is determined from the equation

$$\delta R = \left[\frac{\partial R}{\partial w}\right]\delta w + \left[\frac{\partial R}{\partial S}\right]\delta S = 0$$

Next, introducing a *Lagrange multiplier* or *costate vector* ψ of the same dimension as *w*, we have

$$\begin{aligned} \delta I &= \frac{\partial I^T}{\partial w}\delta w + \frac{\partial I^T}{\partial S}\delta S - \psi^T\left(\left[\frac{\partial R}{\partial w}\right]\delta w + \left[\frac{\partial R}{\partial S}\right]\delta S\right) \\ &= \left\{\frac{\partial I^T}{\partial w} - \psi^T\left[\frac{\partial R}{\partial w}\right]\right\}\delta w + \left\{\frac{\partial I^T}{\partial S} - \psi^T\left[\frac{\partial R}{\partial S}\right]\right\}\delta S \end{aligned} \tag{3.3}$$

Choosing ψ to satisfy the *adjoint equation*

$$\left[\frac{\partial R}{\partial w}\right]^T \psi = \frac{\partial I}{\partial w} \tag{3.4}$$

then the variation of the flow field variables will not explicitly appear in the expression of the cost variation, i.e., δI is directly correlated with the shape variation δS :

$$\delta I = \left\{\frac{\partial I^T}{\partial S} - \psi^T\left[\frac{\partial R}{\partial S}\right]\right\}\delta S \tag{3.5}$$

In flow physics, the constraint *R* is a partial differential operator (i.e., Euler or Navier-Stokes equation), and the adjoint equation (3.4) is a linear partial differential equation of the same dimension, which for a given shape can be solved once the governing equation of flow field is solved. In other words, the gradient of I with respect to an arbitrary number of design variables can be determined with only one solution each of the governing and adjoint equations, without the need for additional flow-field evaluations[16-18].

Notice that the adjoint equation (3.4) is dependent on the choice of the cost function *I*. Moreover, for partial differential problems, the formulation of Eq. (3.4) comprises the adjoint partial differential equation, as well as its values on the boundary of Ω. This will be elucidated for the inlet design problem in later sections.

IV. Inlet Design Using Euler and Adjoint Equations

A. The Euler Equations

The differential form of the Euler equations can be written as

$$\frac{\partial w}{\partial t} + \frac{\partial f_i}{\partial x_i} = 0 \tag{4.1a}$$

where

$$w = \begin{bmatrix} \rho \\ \rho u_1 \\ \rho u_2 \\ \rho u_3 \\ \rho E \end{bmatrix}, \qquad f_i = \begin{bmatrix} \rho u_i \\ \rho u_i u_1 + p\delta_{i1} \\ \rho u_i u_2 + p\delta_{i2} \\ \rho u_i u_3 + p\delta_{i3} \\ \rho u_i H \end{bmatrix}$$

in which u_1, u_2, u_3 are the velocity components, ρ is the density, *E* is the total energy per unit mass, and δ_{ij} is the Kronecker delta function. Also, the pressure *p* and total specific enthalpy (i.e., total enthalpy per unit mass) *H* are given by

$$p = (\gamma - 1)\rho(E - \frac{1}{2}u_i u_i), \qquad H = E + p/\rho \tag{4.1b}$$

Equation (4.1a) has an equivalent version in computational space

$$\frac{\partial W}{\partial t} + \frac{\partial F_i}{\partial \xi_i} = 0 \tag{4.2}$$

where

$$W = J\begin{bmatrix}\rho\\ \rho u_1\\ \rho u_2\\ \rho u_3\\ \rho E\end{bmatrix}, \qquad F_i = J\frac{\partial \xi_i}{\partial x_j} f_j = S_{ij} f_j = J\begin{bmatrix}\rho U_i\\ \rho U_i u_1 + \dfrac{\partial \xi_i}{\partial x_1} p\\ \rho U_i u_2 + \dfrac{\partial \xi_i}{\partial x_2} p\\ \rho U_i u_3 + \dfrac{\partial \xi_i}{\partial x_3} p\\ \rho U_i H\end{bmatrix} \tag{4.3}$$

in which $U_i = \dfrac{\partial \xi_i}{\partial x_j} u_j$ are contravariant velocity components, S_{ij} and K_{ij} are transformation matrices between the Cartesian coordinates x_1, x_2, x_3 of the physical space and the curvilinear coordinates ξ_1, ξ_2, ξ_3 of the computational space (see Fig. 3), with[17,18]

$$K_{ij} = \left[\frac{\partial x_i}{\partial \xi_j}\right] = \frac{\partial \vec{r}}{\partial \xi_j} = \vec{e}_{\xi_j} \ ,$$

$$J = \det(K) \ , \quad K_{ij}^{-1} = \left[\frac{\partial \xi_i}{\partial x_j}\right],$$

$$S_{ij} = JK_{ij}^{-1} = J\frac{\partial \xi_i}{\partial x_j}$$

Equation (4.2) has the following *weak form* [22] (see Appendix A)

$$\int_{\Omega} \frac{\partial \psi^T}{\partial \xi_i} F_i \, d\Omega = \int_{\partial\Omega} n_i \psi^T F_i \, dB \tag{4.4}$$

where dB is the elemental area on the surface of Ω. Correspondingly the variational form of Eq. (4.2) also has a weak form

$$\int_{\Omega} \frac{\partial \psi^T}{\partial \xi_i} \delta F_i \, d\Omega = \int_{\partial\Omega} n_i \psi^T \delta F_i \, dB \tag{4.5}$$

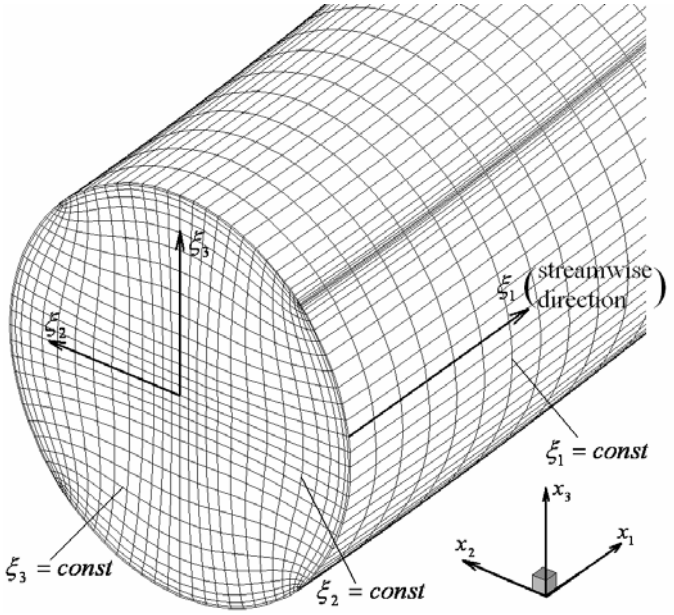

Fig. 3 Cartesian and curvilinear coordinates

where

$$\delta F_i = S_{ij} A_j \delta w + \delta(S_{ij}) f_j = C_i \delta w + \delta(S_{ij}) f_j \tag{4.6a}$$

$$C_i = S_{ij} A_j = JK_{ij}^{-1} A_j = J\frac{\partial \xi_i}{\partial x_j} A_j = J\frac{\partial \xi_i}{\partial x_j}\frac{\partial f_j}{\partial w} \tag{4.6b}$$

$$A_j = \frac{\partial f_j}{\partial w} \tag{4.6c}$$

B. Cost Variation and Adjoint Equation

For s-shaped inlet design optimization, a direct objective would be to minimize the total-pressure loss and non-uniformity on the exit face. However, it was found that an adjoint-equation formulation for such a cost function was rather difficult. For inviscid flow only shock contributes to the total-pressure loss and non-uniformity. In this case, one may attempt to reduce the wall pressure drag in the hope of weakening the shock and, thus, reducing the total-pressure loss and non-uniformity. Thus we shall choose wall pressure drag in the *x*-direction as the cost function. Now, the drag coefficient can be expressed as

$$C_D = C_{F_x} = \frac{F_x}{\frac{1}{2}\rho_\infty q_\infty^2 L^2} = \int_{B_W} -\frac{p}{\frac{1}{2}\rho_\infty q_\infty^2}\frac{dS_x}{L^2} = \int_{B_W} -2\bar{p}d\bar{S}_x$$

where the bars denote non-dimensional variables. In the following, we shall employ non-dimensional variables and, for simplicity of notation, we shall omit the bars.

Without loss of generality we employ an H-H type computational grid (Fig. 3). Let ξ_1 be the streamwise curvilinear direction, ξ_2 the lateral curvilinear direction**,** and ξ_3 the vertical curvilinear direction. There are two families of wall boundaries: $\xi_2 = const$ and $\xi_3 = const$. Then the cost function at zero angle of attack can be expressed as

$$I = C_D = C_{F_x} = \int_{B_W} -2pdS_x = \int_{\xi_2=const} -2pdS_x + \int_{\xi_3=const} -2pdS_x$$

A variation of the shape will cause a variation δw in the flow field, a corresponding variation δp in the pressure, and consequently a variation of the cost function given by

$$\delta I = \int_{\xi_2=const} -2\delta pdS_x + \int_{\xi_3=const} -2\delta pdS_x + \int_{\xi_2=const} -2p\delta(dS_x) + \int_{\xi_3=const} -2p\delta(dS_x) \qquad (4.7)$$

Adding the variation weak form Eq. (4.5) to Eq. (4.7) and substituting δF_i with its expression in Eq. (4.6), we obtain

$$\begin{aligned}\delta I = &\int_{\xi_2=\text{const}} -2\delta pdS_x + \int_{\xi_3=\text{const}} -2\delta pdS_x \\ &+ \int_{\xi_2=\text{const}} -2p\delta(dS_x) + \int_{\xi_3=\text{const}} -2p\delta(dS_x) \\ &- \int_\Omega \left(\frac{\partial \psi^T}{\partial \xi_i} C_i \delta w + \frac{\partial \psi^T}{\partial \xi_i} \delta S_{ij} f_j \right) d\Omega + \int_{\partial\Omega} n_i \psi^T \delta F_i dB\end{aligned} \qquad (4.8)$$

which has the form of Eq. (3.3). In order to eliminate δw explicitly in δI, let ψ satisfy

$$C_i^T \frac{\partial \psi}{\partial \xi_i} = 0 \qquad (4.9)$$

which is the specialization of the adjoint equation (3.4) to the present problem. Then, substituting Eq. (4.9) into Eq. (4.8), δI becomes

$$\begin{aligned}\delta I = &\int_{\xi_2=const} -2\delta p dS_x + \int_{\xi_3=const} -2\delta p dS_x \\ &+ \int_{\xi_2=const} -2p\delta(dS_x) + \int_{\xi_3=const} -2p\delta(dS_x) \\ &- \int_\Omega \frac{\partial \psi^T}{\partial \xi_i} \delta S_{ij} f_j d\Omega + \int_{\partial\Omega} n_i \psi^T \delta F_i dB\end{aligned} \tag{4.10}$$

The next step is to eliminate the variations of flow variables in the boundary integrals of Eq. (4.10) by setting boundary conditions for the adjoint equation (4.9). Conditions on inflow and outflow boundaries are needed only in the last integral of Eq. (4.10). On the entrance inflow boundary ($\xi_1 = 0$), all flow variables are specified for supersonic inflow, so $\delta F_1 = 0$. On the exit outflow boundary ($\xi_1 = \xi_{1\max}$), the coordinate transformation is such that $\delta S_{ij} = \delta(JK_{ij}^{-1})$ is zero in the outflow boundary; in effect, since the optimization leaves the exit face geometry constant, i.e., $S_{1j} = const$, thus $\delta S_{1j} = 0$. Then, $\delta F_1 = C_1 \delta w$ (recall Eq. (4.6a)) at the exit. Consequently one can chooses boundary conditions for ψ such that[17,18]

$$n_i \psi^T C_i \delta w = n_1 \psi^T C_1 \delta w = \psi^T C_1 \delta w = 0$$

Next, on the wall boundaries ($\xi_2 = 0$, $\xi_2 = \xi_{2\max}$, $\xi_3 = 0$, and $\xi_3 = \xi_{3\max}$) the normal velocity components are zero, i.e., $U_i = 0$ $(i = 2,3)$. Hence, the boundary integral $\int_{\partial\Omega} n_i \psi^T \delta F_i dB$ can be greatly simplified and the cost variation becomes (see Appendix B):

$$\begin{aligned}\delta I = &\int_{\xi_2=0} -2\delta p S_{21} d\xi_3 d\xi_1 + \int_{\xi_2=0} -2p\delta(S_{21}) d\xi_3 d\xi_1 \\ &+ \int_{\xi_2=\xi_{2\max}} -2\delta p(-S_{21}) d\xi_3 d\xi_1 + \int_{\xi_2=\xi_{2\max}} -2p\delta(-S_{21}) d\xi_3 d\xi_1 \\ &+ \int_{\xi_3=0} -2\delta p S_{31} d\xi_1 d\xi_2 + \int_{\xi_3=0} -2p\delta(S_{31}) d\xi_1 d\xi_2 \\ &+ \int_{\xi_3=\xi_{3\max}} -2\delta p(-S_{31}) d\xi_1 d\xi_2 + \int_{\xi_3=\xi_{3\max}} -2p\delta(-S_{31}) d\xi_1 d\xi_2 - \int_\Omega \frac{\partial \psi^T}{\partial \xi_i} \delta S_{ij} f_j d\Omega \\ &- \int_{\xi_2=0} J\left(\psi_2 \frac{\partial \xi_2}{\partial x_1} + \psi_3 \frac{\partial \xi_2}{\partial x_2} + \psi_4 \frac{\partial \xi_2}{\partial x_3}\right) \delta p d\xi_3 d\xi_1 - \int_{\xi_2=0} \left(\psi_2 \delta S_{21} + \psi_3 \delta S_{22} + \psi_4 \delta S_{23}\right) p d\xi_3 d\xi_1 \\ &+ \int_{\xi_2=\xi_{2\max}} J\left(\psi_2 \frac{\partial \xi_2}{\partial x_1} + \psi_3 \frac{\partial \xi_2}{\partial x_2} + \psi_4 \frac{\partial \xi_2}{\partial x_3}\right) \delta p d\xi_3 d\xi_1 + \int_{\xi_2=\xi_{2\max}} \left(\psi_2 \delta S_{21} + \psi_3 \delta S_{22} + \psi_4 \delta S_{23}\right) p d\xi_3 d\xi_1 \\ &- \int_{\xi_3=0} J\left(\psi_2 \frac{\partial \xi_3}{\partial x_1} + \psi_3 \frac{\partial \xi_3}{\partial x_2} + \psi_4 \frac{\partial \xi_3}{\partial x_3}\right) \delta p d\xi_1 d\xi_2 - \int_{\xi_3=0} \left(\psi_2 \delta S_{31} + \psi_3 \delta S_{32} + \psi_4 \delta S_{33}\right) p d\xi_1 d\xi_2 \\ &+ \int_{\xi_3=\xi_{3\max}} J\left(\psi_2 \frac{\partial \xi_3}{\partial x_1} + \psi_3 \frac{\partial \xi_3}{\partial x_2} + \psi_4 \frac{\partial \xi_3}{\partial x_3}\right) \delta p d\xi_1 d\xi_2 + \int_{\xi_3=\xi_{3\max}} \left(\psi_2 \delta S_{31} + \psi_3 \delta S_{32} + \psi_4 \delta S_{33}\right) p d\xi_1 d\xi_2\end{aligned} \tag{4.11}$$

By letting ψ satisfy the following wall boundary conditions

$$\psi_2 S_{21} + \psi_3 S_{22} + \psi_4 S_{23} = -2S_{21} \qquad \text{on} \quad \xi_2 = const \tag{4.12a}$$

$$\psi_2 S_{31} + \psi_3 S_{32} + \psi_4 S_{33} = -2S_{31} \qquad \text{on} \quad \xi_3 = const \tag{4.12b}$$

δp is eliminated from the expression of δI :

$$\begin{aligned}\delta I = -\int_\Omega \frac{\partial \psi^T}{\partial \xi_i}\delta S_{ij} f_j d\Omega - \int_{\xi_2=0}\left((2+\psi_2)\delta S_{21}+\psi_3\delta S_{22}+\psi_4\delta S_{23}\right)p d\xi_3 d\xi_1 \\ + \int_{\xi_2=\xi_{2\max}}\left((2+\psi_2)\delta S_{21}+\psi_3\delta S_{22}+\psi_4\delta S_{23}\right)p d\xi_3 d\xi_1 \\ - \int_{\xi_3=0}\left((2+\psi_2)\delta S_{31}+\psi_3\delta S_{32}+\psi_4\delta S_{33}\right)p d\xi_1 d\xi_2 \\ + \int_{\xi_3=\xi_{3\max}}\left((2+\psi_2)\delta S_{31}+\psi_3\delta S_{32}+\psi_4\delta S_{33}\right)p d\xi_1 d\xi_2\end{aligned} \tag{4.13}$$

Equation (4.13) is the final expression of the cost variation in the form of Eq. (3.5), i.e., δI depends only on the variations of the shape δS_{ij}, and this dependence is linear.

V. Design Optimization Process

The general process of design optimization can be summarized as follows:

1° First, input initial shape and the corresponding grid.

2° Second, solve Euler equations.

3° Then, solve the adjoint equation.

4° Find the gradient of the cost function

$$G(k) = \frac{\partial I}{\partial \alpha_k}, \qquad k = 1,2,3,...,N$$

5° Modify the shape by modifying the design variables

$$\alpha_k^{(n+1)} = \alpha_k^{(n)} - \lambda G(k), \qquad k = 1,2,3,...,N$$

6° Stop if the design convergence criteria are satisfied, or else, return to 2°.

The details of the above process are described below.

A. Step 1: Input Initial Shape and the Corresponding Grid

First, a 2-d grid of the unit disc is generated (see Fig. 4). The grid for the initial baseline shape of the form of Eq. (2.1) is obtained by copying this 2-d grid to each cross section of the inlet. When the inlet shape changes subsequently due to changes in the design variables, the new grid for the modified shape is obtained in the same way.

B. Step 2: Solution of the Euler Equations

The Euler equations are discretized by the finite volume method and solved by a Runge-Kutta multistage explicit time-stepping scheme with artificial dissipation, local time step and implicit residual smoothing[23]. The boundary conditions comprise the no-penetration condition on wall surfaces, and boundary values on entrance and exit faces introduced via a characteristic analysis. In the latter, characteristic variables are specified according to the propagation direction of the perturbation waves, except one equation at the exit which is replaced by the condition that the pressure equals the back pressure for subsonic outflow[24-26].

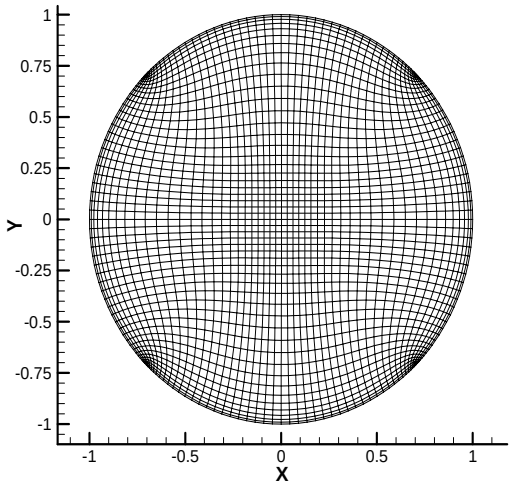

Fig. 4 H-H grid of the disc

C. Step 3: Solution of the Adjoint Equation

To obtain a solution of the costate vector ψ for the adjoint equation (4.9), we note that it can be computed as the steady-state solution of the time-dependent equation:

$$\frac{\partial \psi}{\partial \tau} - C_i^T \frac{\partial \psi}{\partial \xi_i} = 0 \tag{5.1}$$

where τ is a *pseudo time* and only has an artificial meaning. The above equation expressed in computation space is first transformed to the physical space in the following form (see Appendix C)

$$\frac{\partial \psi}{\partial \tau} - A_1^T \frac{\partial \psi}{\partial x} - A_2^T \frac{\partial \psi}{\partial y} - A_3^T \frac{\partial \psi}{\partial z} = 0 \tag{5.2}$$

Integrating this equation in a grid cell $V_{i,j,k}$ with A_1^T , A_2^T , and A_3^T regarded as constants over the cell, and using the Gauss formula, yields the following equation

$$\int_{V_{i,j,k}} \frac{\partial \psi}{\partial \tau} dV - (A_1^T)_{i,j,k} \oint_{S_{i,j,k}} \psi dS_x - (A_2^T)_{i,j,k} \oint_{S_{i,j,k}} \psi dS_y - (A_3^T)_{i,j,k} \oint_{S_{i,j,k}} \psi dS_z = 0 \tag{5.3}$$

where $S_{i,j,k}$ is the outer face of $V_{i,j,k}$. Equation (5.3) can be rewritten as

$$V_{i,j,k}\left(\frac{d\psi}{d\tau}\right) = Q_{i,j,k} \tag{5.4}$$

The boundary conditions include the wall boundary condition, and the entrance and exit boundary conditions. To satisfy the boundary condition Eq. (4.12a) on the wall boundary $\xi_2 = 0$, ψ can be specified as follows

$$\psi_1(i, \frac{1}{2}, k) = \psi_1(i,1,k) \tag{5.5a}$$

$$\begin{aligned}\psi_2(i, \frac{1}{2}, k) = {} & \frac{S_{21}}{S_{21}^2 + S_{22}^2 + S_{23}^2}(-2S_{21}) + \frac{S_{22}^2 + S_{23}^2}{S_{21}^2 + S_{22}^2 + S_{23}^2}\psi_2(i,1,k) \\ & - \frac{S_{21}S_{22}}{S_{21}^2 + S_{22}^2 + S_{23}^2}\psi_3(i,1,k) - \frac{S_{21}S_{23}}{S_{21}^2 + S_{22}^2 + S_{23}^2}\psi_4(i,1,k)\end{aligned} \tag{5.5b}$$

$$\begin{aligned}\psi_3(i, \frac{1}{2}, k) = {} & \frac{S_{22}}{S_{21}^2 + S_{22}^2 + S_{23}^2}(-2S_{21}) - \frac{S_{21}S_{22}}{S_{21}^2 + S_{22}^2 + S_{23}^2}\psi_2(i,1,k) \\ & + \frac{S_{21}^2 + S_{23}^2}{S_{21}^2 + S_{22}^2 + S_{23}^2}\psi_3(i,1,k) - \frac{S_{22}S_{23}}{S_{21}^2 + S_{22}^2 + S_{23}^2}\psi_4(i,1,k)\end{aligned} \tag{5.5c}$$

$$\begin{aligned}\psi_4(i, \frac{1}{2}, k) = {} & \frac{S_{23}}{S_{21}^2 + S_{22}^2 + S_{23}^2}(-2S_{21}) - \frac{S_{21}S_{23}}{S_{21}^2 + S_{22}^2 + S_{23}^2}\psi_2(i,1,k) \\ & - \frac{S_{22}S_{23}}{S_{21}^2 + S_{22}^2 + S_{23}^2}\psi_3(i,1,k) + \frac{S_{21}^2 + S_{22}^2}{S_{21}^2 + S_{22}^2 + S_{23}^2}\psi_4(i,1,k)\end{aligned} \tag{5.5d}$$

$$\psi_5(i,\frac{1}{2},k) = \psi_5(i,1,k) \tag{5.5e}$$

Similarly on the wall boundary $\xi_2 = \xi_{2\max}$. Likewise, ψ is specified to satisfy the wall boundary condition Eq. (4.12b) on $\xi_3 = 0$ and $\xi_3 = \xi_{3\max}$.

Borrowing a physics viewpoint, the implementation of the adjoint boundary conditions on the entrance and exit faces must obey the direction of information propagation because the adjoint equation is a hyperbolic equation. This is done by the following characteristic analysis[19]. Taking the exit outflow boundary ($\xi_1 = \xi_{1\max}$) as an example, at any arbitrary point on the boundary only changes of dependent variables across the boundary in its normal direction (ξ_1 direction) are of interest. Then the time-dependent adjoint equation (5.1) on the exit boundary can be simplified to

$$\frac{\partial \psi}{\partial \tau} - {C_1}^T \frac{\partial \psi}{\partial \xi_1} = 0 \tag{5.6}$$

Let T be the matrix that transforms ${C_1}^T$ to a diagonal matrix D:

$$T^{-1}{C_1}^T T = D$$

and let ϕ be the image of ψ by the same transformation:

$$\psi = T\phi \tag{5.7}$$

Then Eq. (5.6) becomes

$$\frac{\partial}{\partial \tau}(T\phi) - {C_1}^T \frac{\partial}{\partial \xi_1}(T\phi) = 0 \tag{5.8}$$

Since ${C_1}^T$ is composed of the converged Euler flow variables, T is constant with respect to the pseudo time τ. Besides, we assume that $\partial T/\partial \xi_1 = 0$ at the outflow boundary. Thus Eq. (5.8) simplifies to

$$T\frac{\partial \phi}{\partial \tau} - {C_1}^T T \frac{\partial \phi}{\partial \xi_1} = 0 \tag{5.9}$$

Multiplying Eq. (5.9) by T^{-1}, we arrive at

$$\frac{\partial \phi}{\partial \tau} - D\frac{\partial \phi}{\partial \xi_1} = 0 \tag{5.10}$$

where

$$D = \begin{bmatrix} \delta_1 & & & & \\ & \delta_2 & & O & \\ & & \delta_3 & & \\ & O & & \delta_4 & \\ & & & & \delta_5 \end{bmatrix}$$

or we can rewrite Eq. (5.10) as

$$\frac{\partial \phi_i}{\partial \tau} - \delta_i \frac{\partial \phi_i}{\partial \xi_1} = 0, \qquad (i = 1,2,3,4,5) \tag{5.11}$$

The solution of Eq. (5.11) has the form

$$\phi_i = f_i(\xi_1 + \delta_i \tau), \qquad (i = 1,2,3,4,5) \tag{5.12}$$

If δ_i >0, the slope of the characteristic line is negative, i.e., the wave propagates inward, and the boundary value ϕ_{iB} should take values from the outside. Thus, we specify zero boundary value for this case: $\phi_{iB} = 0$. If δ_i <0, the slope of the characteristic line is positive, i.e., the wave propagates outward, and ϕ_{iB} should take values by extrapolation from inside the flow field: $\phi_{iB} = \phi_i^e$, where ϕ_i^e is the value of ϕ_i extrapolated from interior field. In summary,

$$\phi_{iB} = \beta_i \phi_i^e \tag{5.13}$$

where

$$\beta_i = \begin{cases} 0, & if \quad \delta_i > 0 \\ 1, & if \quad \delta_i < 0 \end{cases} \tag{5.14}$$

Finally, the boundary values of the original costate is obtained by $\psi_B = T\phi_B$.

On the entrance inflow boundary, the outward normal of the boundary face is in the negative direction of ξ_1. Hence, the reverse of Eq. (5.14) can be applied.

As in solving Euler equations, artificial dissipation is also needed here to make the time stepping stable

$$\frac{d\psi_{i,j,k}}{d\tau} = R_{i,j,k} = \frac{1}{V_{i,j,k}}\left(Q_{i,j,k} + D_{i,j,k}\right) \tag{5.15}$$

The same Runge-Kutta three-stage explicit time stepping scheme as in Step 2 is used to iterate this equation to a steady solution with local time step and implicit residual smoothing[19].

D. Step 4: Calculation of the Cost Gradient

After solving the Euler equations and the adjoint equation in each design cycle, the flow variables f_i and the costate vector ψ are known. We then calculate the variation of the cost function and its gradient as follows:

1) Keep all except the k^{th} design variables unchanged, i.e., add a small variation to the k^{th} design variable:

$$\alpha_k^{new} = \alpha_k^{old} + \delta\alpha_k$$

so that the shape undergoes a small variation corresponding to $\delta\alpha_k$. Here $\delta\alpha_k$ should be sufficiently small.

2) Create a new grid ($x_{i,j}^{new}$, $y_{i,j}^{new}$) corresponding to the new shape.

3) Calculate the variation of the metric terms in the expression of δI :

$$\delta S_{ij} = S_{ij}^{new} - S_{ij}^{old}$$

where S_{ij}^{new} and S_{ij}^{old} are calculated from the new and old grids, respectively.

4) Calculate the integrals in the expression of δI and obtain the k^{th} component of the gradient

$$G(k) = \frac{\partial I}{\partial \alpha_k} = \frac{\delta I}{\delta \alpha_k}$$

5) Calculate all the components of *G* similarly.

It is important to note that the above process involves purely algebraic operations, and the Euler and adjoint equations need not be recomputed in this step.

E. Step 5: Shape Modification

The shape for the next design cycle is obtained by modifying the design variables in the negative gradient direction:

$$\alpha_k^{(n+1)} = \alpha_k^{(n)} - \lambda G(k), \quad k = 1,2,3,..., N$$

where *G* is, in fact, normalized by the absolute value of its maximum component in magnitude when used above in shape modification. In addition, we employ an adaptive step size λ to ensure the algorithm does not overstep a minimum. With the newly-updated design variables, the inlet shape is modified by changing its centerline shape and its radius distribution function according to Eq. (2.2).

F. Step 6: Convergence Criterion

Since we adopt an adaptive step size, the algorithm is considered to have converged if the step size has been reduced to below a threshold without further improving the cost function. Otherwise, the algorithm loops to Step 2.

VI. Results and Discussions

In the result presented below, we have selected a baseline shape defined by the following centerline and radius distribution:

$$\frac{z_{baseline}}{s} = 3\left(\frac{x}{L}\right)^2 - 2\left(\frac{x}{L}\right)^3 \qquad (6.1a)$$

$$\frac{r_{baseline} - r_1}{r_2 - r_1} = 3\left(\frac{x}{L}\right)^2 - 2\left(\frac{x}{L}\right)^3 \qquad (6.1b)$$

with entrance radius $r_1 = 0.5$, exit radius $r_2 = 0.75$, length L=12, and centerline offset $s = 2$, as shown in Fig. 5. For this design we set the freestream Mach number to be 1.5, the exit back pressure to $p_b = 0.8 p_t^{in}$, where p_t^{in} is the total pressure of free stream flow. The value of p_b thus chosen is high enough to obtain subsonic flow at the exit.

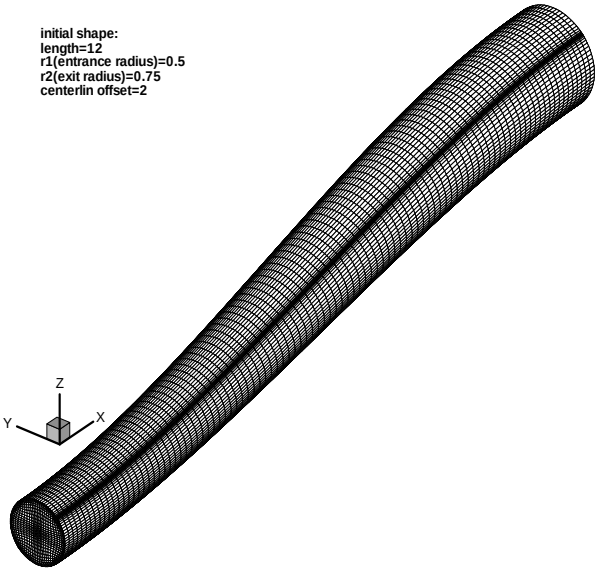

Fig. 5 Initial (baseline) shape

Fig. 6 and Fig. 7 show the convergence history of the Euler and adjoint solvers for the initial shape. Convergence trends for the subsequent shapes are similar. The optimization algorithm in Section 5 is performed over 28 cycles. Fig. 8(a) and Fig. 8(b) show the history of the cost function, i.e., wall pressure drag, and the adaptive

step size. The optimization is halted as the latter descends sharply after 26 cycles, meaning that the algorithm has reached a local minimum of the cost function. From the figures we can see that drag is effectively reduced.

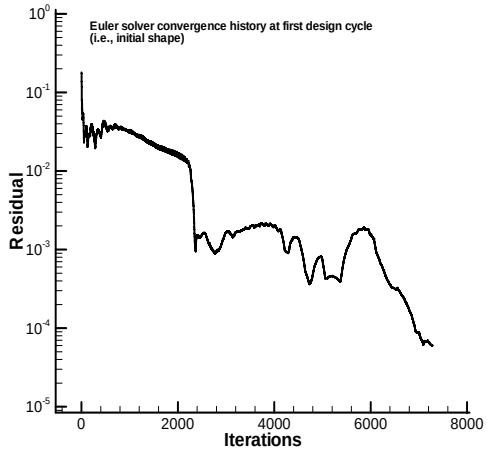

Fig. 6 Euler solver convergence history

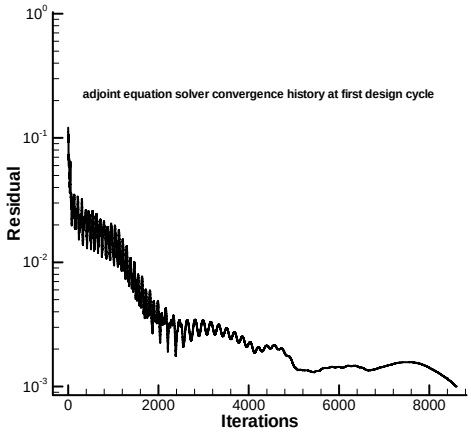

Fig. 7 Adjoint solver convergence history

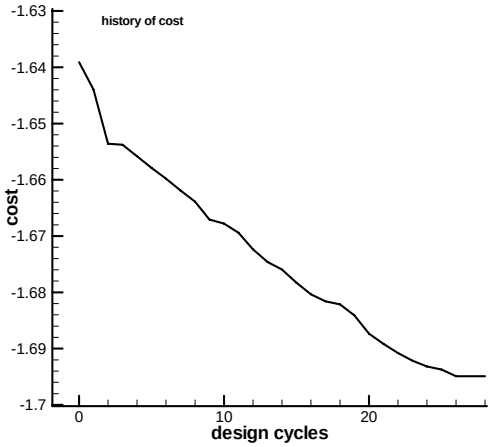

Fig. 8(a) History of cost function

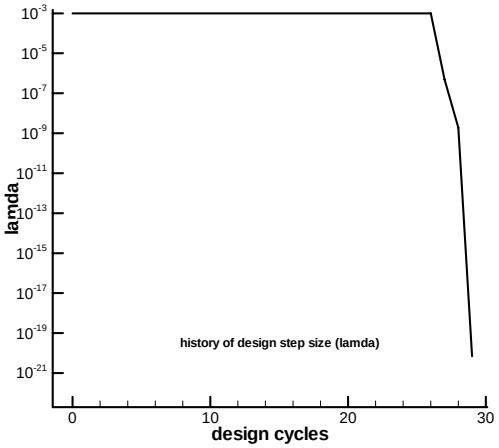

Fig. 8(b) History of adaptive step size

As mentioned in the introduction, wall pressure drag is only an indirect cost function. Rather, for practical design, one would be more interested in the average total pressure on the exit face:

$$p_t^{avr} = \left(\sum_{k=1}^{K_m} \sum_{j=1}^{J_m} \Delta S_{j,k}\, p_{t\,j,k} \right) \Bigg/ \left(\sum_{k=1}^{K_m} \sum_{j=1}^{J_m} \Delta S_{j,k} \right) \tag{6.2}$$

as well as the quadratic mean deviation thus measures the non-uniformity of total pressure distribution on the exit face:

$$p_t^{sqd} = \sqrt{\left(\sum_{k=1}^{K_m} \sum_{j=1}^{J_m} \Delta S_{j,k} (p_{t\,j,k} - p_t^{avr})^2 \right) \Bigg/ \left(\sum_{k=1}^{K_m} \sum_{j=1}^{J_m} \Delta S_{j,k} \right)} \tag{6.3}$$

In the above definitions, $\Delta S_{j,k}$ is the area of each grid cell on exit face, $K_m \times J_m$ is the total number of grid cells. Fig. 8(c) shows that the quadratic mean deviation is reduced by about 28% as a result of the optimization, which means that uniformity of total pressure is indeed improved in this approach. However, Fig. 8(d) shows that further loss of about 1% is incurred in the average total pressure. This result suggests that, with the indirect approach of minimizing drag, one cannot at the same time improve pressure uniformity as well as average total pressure, although loss of the latter is small.

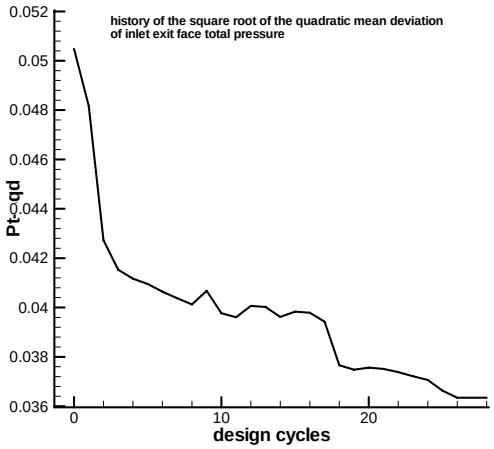

Fig. 8(c) History of the quadratic mean deviation of exit total pressure

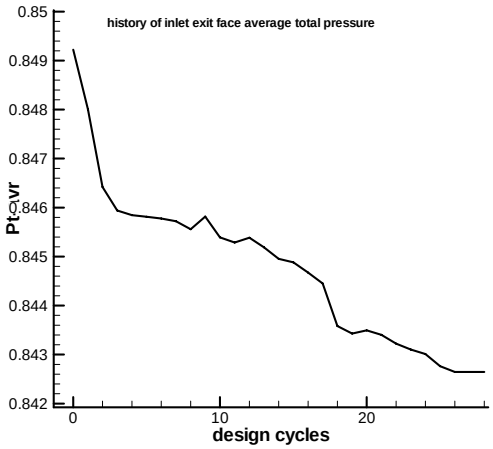

Fig. 8(d) History of exit average total pressure

A comparison of exit face total pressure contours of initial and final shape in Fig. 9 and Fig. 10 indicates that both the areas of the lowest and highest total pressures are reduced, that is, the total pressure distribution becomes

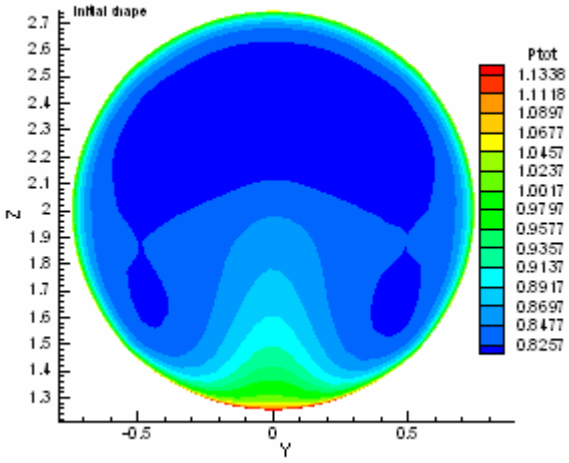

Fig. 9 Initial p_t contours on exit face

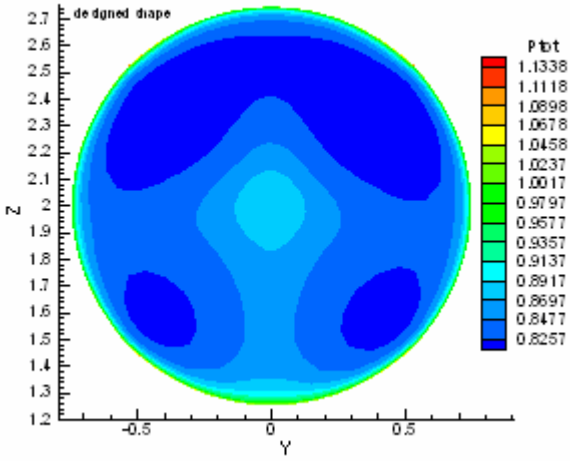

Fig. 10 Designed p_t contours on exit face

more uniform as a result of optimization. The same conclusion can be formed by comparing the interior field total-pressure contours of the initial shape (Fig. 11) and those of the final shape (Fig. 12). From these two figures it can be seen that the flow is compressed through a series of compression waves. After optimization, the maximum total-pressure of the final shape is reduced, whereas the minimum is increased by some amount in the interior field.

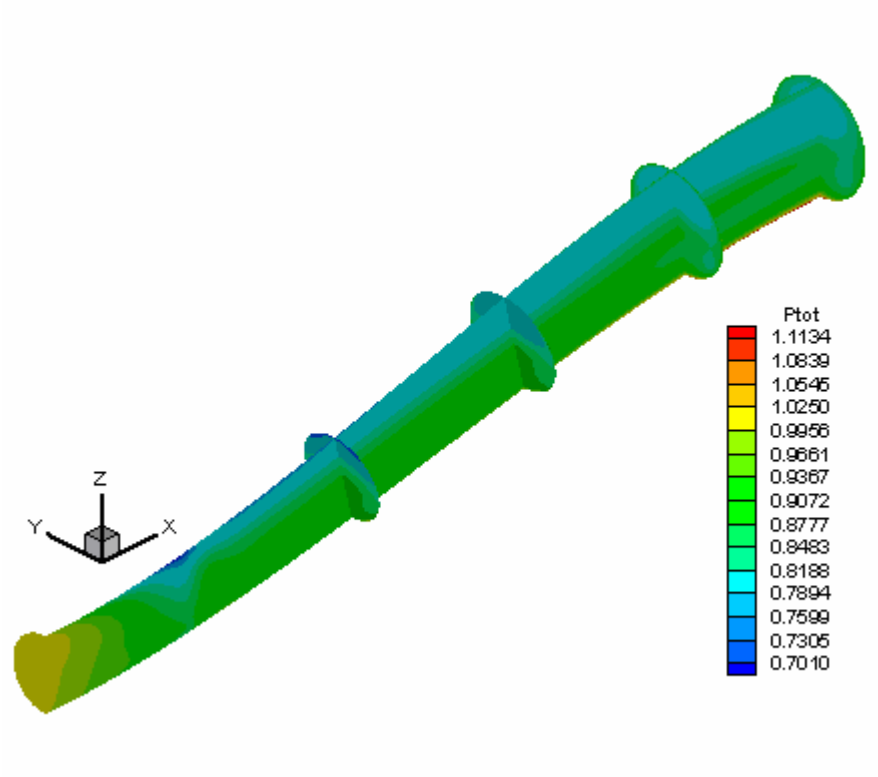

Fig. 11 Initial shape total pressure contours

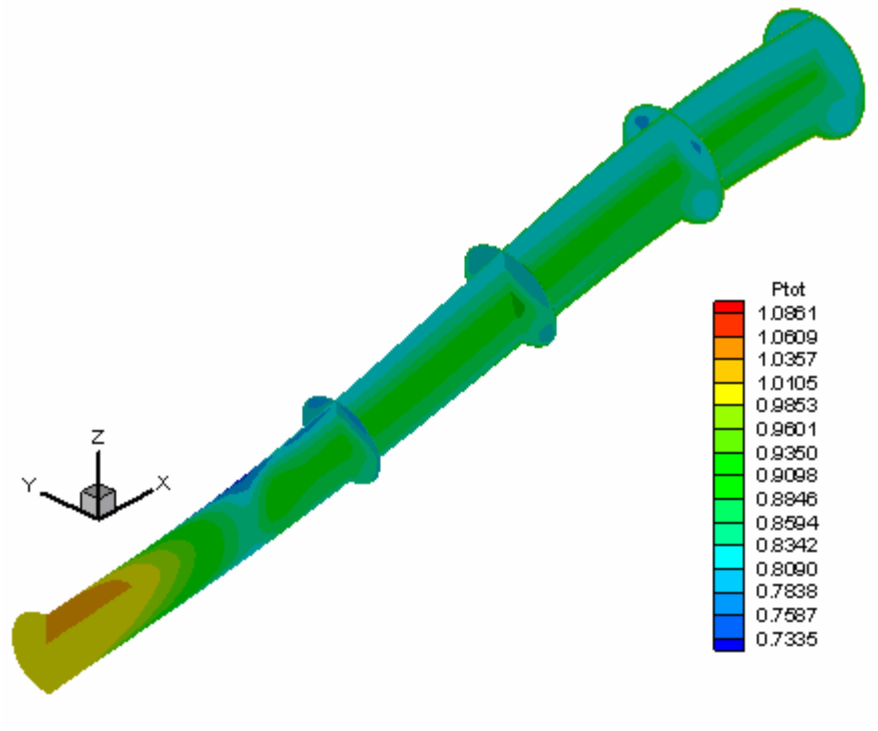

Fig.12 Designed shape total pressure contours

Finally, Fig. 13 compares the initial shape and the final shape at the end of 28 design cycles. The shape is modified significantly, and primarily immediately after the entrance.

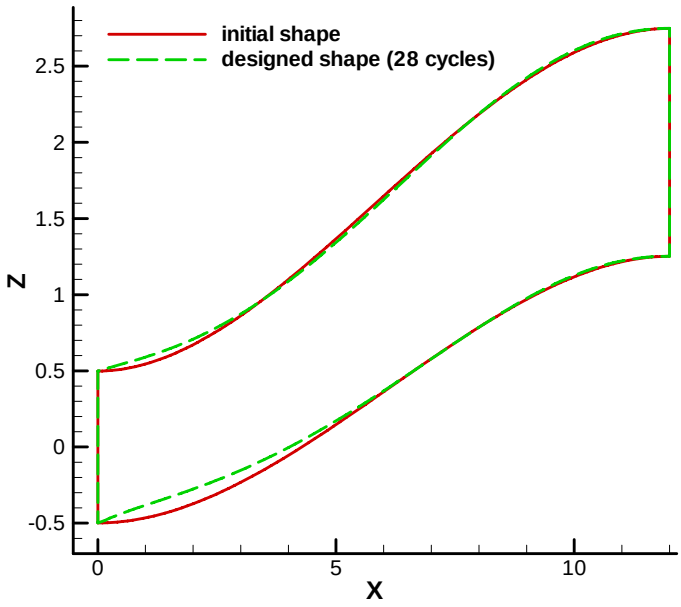

Fig. 13 Initial shape and designed shape

VII. Conclusions

In this paper, the adjoint equation method was applied to the optimization of an s-shaped duct representing an engine inlet. A practical design purpose would be to minimize the exit face total-pressure distortion (i.e., non-uniformity) without loss in total pressure. However, this would lead to inextricable adjoint equations. As an alternate, we have adopted an indirect way consisting in taking the wall pressure drag as cost function. The design process shows that as drag is reduced, the total pressure at the exit face indeed becomes more uniform. However, the exit face average total pressure is slightly decreased as a result. Compared to large scale optimization using evolutionary strategies, the adjoint method is visibly less costly in computation time, although it can only arrive at a local optimum. Nevertheless, the study shows that the presented approach is useful for improving an initial baseline design. This study considers only inviscid flow, i.e., effect of pressure drag on inlet performance. Future study should further consider viscous flow to account for friction drag[27], and possibly direct numerical simulation (DNS)[28] to better model the complex flow in an inlet.

Appendix A. The Weak Form of Euler Equations

A.1 The Weak Form of Euler Equations in Physical Space

The conservative Euler equations in integral form can be written as

$$\frac{\partial}{\partial t}\int_V w dV + \int_{\partial V} \vec{f}\cdot d\vec{S} = 0 \qquad \text{(A-1)}$$

where ∂V is the boundary of volume domain V, $d\vec{S}$ is the vectored elemental area on the surface of V with its direction pointing in outward normal direction and

$$w = \begin{bmatrix} \rho \\ \rho u_1 \\ \rho u_2 \\ \rho u_3 \\ \rho E \end{bmatrix} \qquad \vec{f} = \begin{bmatrix} \rho u_1 & \rho u_2 & \rho u_3 \\ \rho u_1 u_1 + p & \rho u_2 u_1 & \rho u_3 u_1 \\ \rho u_1 u_2 & \rho u_2 u_2 + p & \rho u_3 u_2 \\ \rho u_1 u_3 & \rho u_2 u_3 & \rho u_3 u_3 + p \\ \rho u_1 H & \rho u_2 H & \rho u_3 H \end{bmatrix}$$

$$p = (\gamma - 1)\rho(E - \frac{1}{2} u_i u_i) \qquad H = E + p/\rho$$

Using Gauss formula to transform the second term in Eq. (A-1) into volume integral, we obtain

$$\frac{\partial}{\partial t} \int_V w dV + \int_V (\nabla \cdot \vec{f}) dV = 0$$

Since the integral is independent of the size of the volume domain V , we then get

$$\frac{\partial w}{\partial t} + \nabla \cdot \vec{f} = 0 \tag{A-2}$$

The above equation is the conservative differential form of Euler equations. Multiply each of Eq. (A-2) with any differentiable function $\varphi_i \quad (i = 1,2,3,4,5)$ and integrate over V

$$\int_V \varphi^T \frac{\partial w}{\partial t} dV + \int_V \varphi^T \nabla \cdot \vec{f} dV = 0 \tag{A-3}$$

where $\varphi = (\varphi_1, \varphi_2, \varphi_3, \varphi_4, \varphi_5)^T$. Using the vector operation formula

$$\nabla \cdot (\varphi^T \vec{f}) = \varphi^T \nabla \cdot \vec{f} + (\nabla \varphi^T) \cdot \vec{f}$$

while being aware of that the gradient operator ∇ acts only on φ^T in the term $(\nabla \varphi^T) \cdot \vec{f}$, then Eq. (A-3) becomes

$$\int_V \varphi^T \frac{\partial w}{\partial t} dV + \int_V \nabla \cdot (\varphi^T \vec{f}) dV - \int_V (\nabla \varphi^T) \cdot \vec{f} dV = 0$$

Using Gauss formula in the above equation, we arrive at

$$\int_V \varphi^T \frac{\partial w}{\partial t} dV = \int_V (\nabla \varphi^T) \cdot \vec{f} dV - \int_{\partial V} \varphi^T \vec{f} \cdot d\vec{S} \tag{A-4}$$

This equation is called the weak form of Euler equations[22]. For steady flows, Eq. (A-4) simplifies to

$$\int_V (\nabla \varphi^T) \cdot \vec{f} dV = \int_{\partial V} \varphi^T \vec{f} \cdot d\vec{S} \tag{A-5}$$

If we write Eq. (A-2) in tensor form

$$\frac{\partial w}{\partial t} + \frac{\partial f_i}{\partial x_i} = 0 \tag{A-6}$$

where

$$f_i = \begin{bmatrix} \rho u_i \\ \rho u_i u_1 + p\delta_{i1} \\ \rho u_i u_2 + p\delta_{i2} \\ \rho u_i u_3 + p\delta_{i3} \\ \rho u_i H \end{bmatrix}$$

correspondingly we can write the following terms in tensor form:

$$(\nabla \varphi^T) \cdot \vec{f} = (\frac{\partial \varphi^T}{\partial x_1}, \frac{\partial \varphi^T}{\partial x_2}, \frac{\partial \varphi^T}{\partial x_3}) \cdot (f_1, f_2, f_3) = \frac{\partial \varphi^T}{\partial x_1} f_1 + \frac{\partial \varphi^T}{\partial x_2} f_2 + \frac{\partial \varphi^T}{\partial x_3} f_3 = \frac{\partial \varphi^T}{\partial x_j} f_j$$

$$\varphi^T \vec{f} \cdot d\vec{S} = \varphi^T (f_1 n_1 + f_2 n_2 + f_3 n_3) dS = \varphi^T f_i n_i dS$$

Thus Eq. (A-5) can be written as

$$\int_V \frac{\partial \varphi^T}{\partial x_j} f_j dV = \int_{\partial V} n_i \varphi^T f_i dS \tag{A-7}$$

A.2 The Weak Form of Euler Equations in Computational Space

Consider a transformation from Cartesian coordinates x_1, x_2, x_3 (physical space) to coordinates ξ_1, ξ_2, ξ_3 (computational space) where

$$K_{ij} = \left[\frac{\partial x_i}{\partial \xi_j}\right] = \frac{\partial \vec{r}}{\partial \xi_j} = \vec{e}_{\xi_j}, \quad J = \det(K), \quad K_{ij}^{-1} = \left[\frac{\partial \xi_i}{\partial x_j}\right] = \nabla \xi_i = \vec{e}^{\,i}, \quad S_{ij} = JK_{ij}^{-1} = J\frac{\partial \xi_i}{\partial x_j}$$

Introduce the contravariant velocity components as[17,18]

$$U_i = \frac{\partial \xi_i}{\partial x_j} u_j$$

The Euler equations can then be written in computational domain as

$$\frac{\partial W}{\partial t} + \frac{\partial F_i}{\partial \xi_i} = 0 \tag{A-8}$$

with

$$W = J\begin{bmatrix}\rho\\ \rho u_1\\ \rho u_2\\ \rho u_3\\ \rho E\end{bmatrix}, \qquad F_i = J\frac{\partial \xi_i}{\partial x_j} f_j = S_{ij} f_j = J\begin{bmatrix}\rho U_i\\ \rho U_i u_1 + \dfrac{\partial \xi_i}{\partial x_1} p\\ \rho U_i u_2 + \dfrac{\partial \xi_i}{\partial x_2} p\\ \rho U_i u_3 + \dfrac{\partial \xi_i}{\partial x_3} p\\ \rho U_i H\end{bmatrix}$$

Analogous to Eq. (A-6) the computational domain Euler equations Eq. (A-8) have a weak form in computational space, similar to Eq. (A-7):

$$\int_\Omega \frac{\partial \varphi^T}{\partial \xi_i} F_i d\Omega = \int_{\partial\Omega} n_i \varphi^T F_i dB \tag{A-9}$$

where dB is the elemental area on the surface of Ω. But here we must keep in mind that the integrals in Eq. (A-9) are performed in computational space (domain).

Take a variation of Eq. (A-8), i.e.,

$$\frac{\partial}{\partial t}(\delta W) + \frac{\partial}{\partial \xi_i}(\delta F)_i = 0$$

Similarly, this equation also has a weak form:

$$\int_\Omega \frac{\partial \varphi^T}{\partial \xi_i} \delta F_i d\Omega = \int_{\partial\Omega} n_i \varphi^T \delta F_i dB \tag{A-10}$$

If the geometry shape of boundaries has a small variation, the whole flow field will have a variation δw, then f_i will have a variation δf_i, and F_i will have a δF_i

$$\delta F_i = \delta(S_{ij} f_j) = S_{ij}\delta f_j + \delta(S_{ij}) f_j$$

Now, let

$$A_j = \frac{\partial f_j}{\partial w}$$

Then

$$\delta f_j = \frac{\partial f_j}{\partial w}\delta w = A_j \delta w$$

Finally

$$\delta F_i = S_{ij} A_j \delta w + \delta(S_{ij}) f_j = C_i \delta w + \delta(S_{ij}) f_j \tag{A-11}$$

where

$$C_i = S_{ij} A_j = J K_{ij}^{-1} A_j = J \frac{\partial \xi_i}{\partial x_j} A_j = J \frac{\partial \xi_i}{\partial x_j} \frac{\partial f_j}{\partial w}$$

Appendix B. Simplification of Cost Variation and Boundary Integrals

The cost variation is expressed as

$$\begin{aligned} \delta I = & \int_{\xi_2=const} -2\delta p dS_x + \int_{\xi_3=const} -2\delta p dS_x \\ & + \int_{\xi_2=const} -2p\delta(dS_x) + \int_{\xi_3=const} -2p\delta(dS_x) \\ & - \int_\Omega \frac{\partial \psi^T}{\partial \xi_i} \delta S_{ij} f_j d\Omega + \int_{\partial\Omega} n_i \psi^T \delta F_i dB \end{aligned} \tag{B-1}$$

The integral on boundary in Eq. (B-1) is

$$\begin{aligned} \int_{\partial\Omega} n_i \psi^T \delta F_i dB = & \int_{\xi_1=0} n_i \psi^T \delta F_i d\xi_2 d\xi_3 + \int_{\xi_1=\xi_{1\max}} n_i \psi^T \delta F_i d\xi_2 d\xi_3 \\ & + \int_{\xi_2=0} n_i \psi^T \delta F_i d\xi_3 d\xi_1 + \int_{\xi_2=\xi_{2\max}} n_i \psi^T \delta F_i d\xi_3 d\xi_1 \\ & + \int_{\xi_3=0} n_i \psi^T \delta F_i d\xi_1 d\xi_2 + \int_{\xi_3=\xi_{3\max}} n_i \psi^T \delta F_i d\xi_1 d\xi_2 \end{aligned} \tag{B-2}$$

Notice that on boundary $\xi_1 = const$, $n_1 = \pm 1, n_2 = n_3 = 0$, on boundary $\xi_2 = const$, $n_2 = \pm 1, n_3 = n_1 = 0$, and on $\xi_3 = const$, $n_3 = \pm 1, n_1 = n_2 = 0$, the boundary integral becomes

$$\begin{aligned} \int_{\partial\Omega} n_i \psi^T \delta F_i dB = & -\int_{\xi_1=0} \psi^T \delta F_1 d\xi_2 d\xi_3 + \int_{\xi_1=\xi_{1\max}} \psi^T \delta F_1 d\xi_2 d\xi_3 \\ & - \int_{\xi_2=0} \psi^T \delta F_2 d\xi_3 d\xi_1 + \int_{\xi_2=\xi_{2\max}} \psi^T \delta F_2 d\xi_3 d\xi_1 \\ & - \int_{\xi_3=0} \psi^T \delta F_3 d\xi_1 d\xi_2 + \int_{\xi_3=\xi_{3\max}} \psi^T \delta F_3 d\xi_1 d\xi_2 \end{aligned} \tag{B-3}$$

In the equation, $\xi_1 = 0, \xi_1 = \xi_{1\max}$ represent the inlet entrance inflow boundary, exit outflow boundary, respectively, while $\xi_2 = 0, \xi_2 = \xi_{2\max}$, $\xi_3 = 0, \xi_3 = \xi_{3\max}$ represent the four wall boundaries. On the entrance boundary ($\xi_1 = 0$), for supersonic inflow, all variables are specified, so $\delta F_i = 0$. On the exit boundary ($\xi_1 = \xi_{1\max}$), incoming characteristics for ψ correspond to outgoing characteristics for δw. Consequently one can choose boundary conditions for ψ such that[17-18]

$$n_i \psi^T C_i \delta w = n_1 \psi^T C_1 \delta w = \psi^T C_1 \delta w = 0$$

On the other hand, if the coordinate transformation is such that $\delta S_{ij} = \delta(JK_{ij}^{-1})$ is negligible in the outflow boundary (in fact, since the inlet exit face geometry makes no change in the optimization process, i.e., $S_{1j} = const$, then $\delta S_{1j} = 0$), thus

$$\psi^T \delta F_1\Big|_{\xi_1=\xi_{1\max}} = \psi^T \delta F_1\Big|_{exit} = \psi^T \left\{C_1 \delta w + \delta(S_{1j}) f_j\right\}\Big|_{exit} = 0$$

Then the boundary integral simplifies to

$$\begin{aligned}\int_{\partial\Omega} n_i \psi^T \delta F_i dB = &-\int_{\xi_2=0} \psi^T \delta F_2 d\xi_3 d\xi_1 + \int_{\xi_2=\xi_{2\max}} \psi^T \delta F_2 d\xi_3 d\xi_1 \\ &-\int_{\xi_3=0} \psi^T \delta F_3 d\xi_1 d\xi_2 + \int_{\xi_3=\xi_{3\max}} \psi^T \delta F_3 d\xi_1 d\xi_2\end{aligned} \tag{B-4}$$

At wall boundaries the normal velocities are zero, i.e., $U_i = 0, (i = 2,3)$, then

$$F_i = J\begin{bmatrix} \rho U_i \\ \rho U_i u_1 + \dfrac{\partial \xi_i}{\partial x_1} p \\ \rho U_i u_2 + \dfrac{\partial \xi_i}{\partial x_2} p \\ \rho U_i u_3 + \dfrac{\partial \xi_i}{\partial x_3} p \\ \rho U_i H \end{bmatrix} = \begin{bmatrix} 0 \\ J\dfrac{\partial \xi_i}{\partial x_1} p \\ J\dfrac{\partial \xi_i}{\partial x_2} p \\ J\dfrac{\partial \xi_i}{\partial x_3} p \\ 0 \end{bmatrix}, \qquad \delta F_i = \begin{bmatrix} 0 \\ J\dfrac{\partial \xi_i}{\partial x_1} \delta p \\ J\dfrac{\partial \xi_i}{\partial x_2} \delta p \\ J\dfrac{\partial \xi_i}{\partial x_3} \delta p \\ 0 \end{bmatrix} + \begin{bmatrix} 0 \\ p\delta(S_{i1}) \\ p\delta(S_{i2}) \\ p\delta(S_{i3}) \\ 0 \end{bmatrix}$$

Thus boundary integral becomes

$$\begin{aligned}&\int_{\partial\Omega} n_i \psi^T \delta F_i dB = \\ &-\int_{\xi_2=0} J\left(\psi_2 \frac{\partial \xi_2}{\partial x_1} + \psi_3 \frac{\partial \xi_2}{\partial x_2} + \psi_4 \frac{\partial \xi_2}{\partial x_3}\right)\delta p d\xi_3 d\xi_1 - \int_{\xi_2=0} \left(\psi_2 \delta S_{21} + \psi_3 \delta S_{22} + \psi_4 \delta S_{23}\right) p d\xi_3 d\xi_1 \\ &+\int_{\xi_2=\xi_{2\max}} J\left(\psi_2 \frac{\partial \xi_2}{\partial x_1} + \psi_3 \frac{\partial \xi_2}{\partial x_2} + \psi_4 \frac{\partial \xi_2}{\partial x_3}\right)\delta p d\xi_3 d\xi_1 + \int_{\xi_2=\xi_{2\max}} \left(\psi_2 \delta S_{21} + \psi_3 \delta S_{22} + \psi_4 \delta S_{23}\right) p d\xi_3 d\xi_1 \\ &-\int_{\xi_3=0} J\left(\psi_2 \frac{\partial \xi_3}{\partial x_1} + \psi_3 \frac{\partial \xi_3}{\partial x_2} + \psi_4 \frac{\partial \xi_3}{\partial x_3}\right)\delta p d\xi_1 d\xi_2 - \int_{\xi_3=0} \left(\psi_2 \delta S_{31} + \psi_3 \delta S_{32} + \psi_4 \delta S_{33}\right) p d\xi_1 d\xi_2 \\ &+\int_{\xi_3=\xi_{3\max}} J\left(\psi_2 \frac{\partial \xi_3}{\partial x_1} + \psi_3 \frac{\partial \xi_3}{\partial x_2} + \psi_4 \frac{\partial \xi_3}{\partial x_3}\right)\delta p d\xi_1 d\xi_2 + \int_{\xi_3=\xi_{3\max}} \left(\psi_2 \delta S_{31} + \psi_3 \delta S_{32} + \psi_4 \delta S_{33}\right) p d\xi_1 d\xi_2\end{aligned} \tag{B-5}$$

Then δI becomes

$$\delta I = \int_{\xi_2=const} -2\delta p dS_x + \int_{\xi_2=const} -2p\delta(dS_x)$$
$$+ \int_{\xi_3=const} -2\delta p dS_x + \int_{\xi_3=const} -2p\delta(dS_x) - \int_\Omega \frac{\partial \psi^T}{\partial \xi_i} \delta S_{ij} f_j d\Omega$$
$$- \int_{\xi_2=0} J\left(\psi_2 \frac{\partial \xi_2}{\partial x_1} + \psi_3 \frac{\partial \xi_2}{\partial x_2} + \psi_4 \frac{\partial \xi_2}{\partial x_3}\right)\delta p d\xi_3 d\xi_1 - \int_{\xi_2=0} \left(\psi_2 \delta S_{21} + \psi_3 \delta S_{22} + \psi_4 \delta S_{23}\right) p d\xi_3 d\xi_1$$
$$+ \int_{\xi_2=\xi_{2\max}} J\left(\psi_2 \frac{\partial \xi_2}{\partial x_1} + \psi_3 \frac{\partial \xi_2}{\partial x_2} + \psi_4 \frac{\partial \xi_2}{\partial x_3}\right)\delta p d\xi_3 d\xi_1 + \int_{\xi_2=\xi_{2\max}} \left(\psi_2 \delta S_{21} + \psi_3 \delta S_{22} + \psi_4 \delta S_{23}\right) p d\xi_3 d\xi_1$$
$$- \int_{\xi_3=0} J\left(\psi_2 \frac{\partial \xi_3}{\partial x_1} + \psi_3 \frac{\partial \xi_3}{\partial x_2} + \psi_4 \frac{\partial \xi_3}{\partial x_3}\right)\delta p d\xi_1 d\xi_2 - \int_{\xi_3=0} \left(\psi_2 \delta S_{31} + \psi_3 \delta S_{32} + \psi_4 \delta S_{33}\right) p d\xi_1 d\xi_2$$
$$+ \int_{\xi_3=\xi_{3\max}} J\left(\psi_2 \frac{\partial \xi_3}{\partial x_1} + \psi_3 \frac{\partial \xi_3}{\partial x_2} + \psi_4 \frac{\partial \xi_3}{\partial x_3}\right)\delta p d\xi_1 d\xi_2 + \int_{\xi_3=\xi_{3\max}} \left(\psi_2 \delta S_{31} + \psi_3 \delta S_{32} + \psi_4 \delta S_{33}\right) p d\xi_1 d\xi_2 \quad \text{(B-6)}$$

Note the transformation relations between the contra-variant base vectors and the covariant base vectors of curvilinear coordinate system

$$\nabla \xi_1 = \frac{1}{J}(\vec{e}_2 \times \vec{e}_3) = \frac{1}{J}(\frac{\partial \vec{r}}{\partial \xi_2} \times \frac{\partial \vec{r}}{\partial \xi_3})$$

$$\nabla \xi_2 = \frac{1}{J}(\vec{e}_3 \times \vec{e}_1) = \frac{1}{J}(\frac{\partial \vec{r}}{\partial \xi_3} \times \frac{\partial \vec{r}}{\partial \xi_1})$$

$$\nabla \xi_3 = \frac{1}{J}(\vec{e}_1 \times \vec{e}_2) = \frac{1}{J}(\frac{\partial \vec{r}}{\partial \xi_1} \times \frac{\partial \vec{r}}{\partial \xi_2})$$

the vectored elemental area on $\xi_2 = const$ boundary and $\xi_3 = const$ boundary can be expressed as, respectively

$$d\vec{S}\Big|_{\xi_2=const} = \pm(\frac{\partial \vec{r}}{\partial \xi_3} \times \frac{\partial \vec{r}}{\partial \xi_1}) d\xi_3 d\xi_1 = \pm J \nabla \xi_2 d\xi_3 d\xi_1 = \pm S_{2j} d\xi_3 d\xi_1$$

$$d\vec{S}\Big|_{\xi_3=const} = \pm(\frac{\partial \vec{r}}{\partial \xi_1} \times \frac{\partial \vec{r}}{\partial \xi_2}) d\xi_1 d\xi_2 = \pm J \nabla \xi_3 d\xi_1 d\xi_2 = \pm S_{3j} d\xi_1 d\xi_2$$

Correspondingly, the projections of the vectored areas in x direction are respectively

$$dS_x\Big|_{\xi_2=const} = d\vec{S} \cdot \vec{i}\Big|_{\xi_2=const} = \pm S_{21} d\xi_3 d\xi_1$$

$$dS_x\Big|_{\xi_3=const} = d\vec{S} \cdot \vec{i}\Big|_{\xi_3=const} = \pm S_{31} d\xi_1 d\xi_2$$

Then δI can be written as

$$\begin{aligned}
\delta I = & \int_{\xi_2=0} -2\delta p S_{21} d\xi_3 d\xi_1 + \int_{\xi_2=0} -2p\delta(S_{21}) d\xi_3 d\xi_1 \\
& + \int_{\xi_2=\xi_{2\max}} -2\delta p(-S_{21}) d\xi_3 d\xi_1 + \int_{\xi_2=\xi_{2\max}} -2p\delta(-S_{21}) d\xi_3 d\xi_1 \\
& + \int_{\xi_3=0} -2\delta p S_{31} d\xi_1 d\xi_2 + \int_{\xi_3=0} -2p\delta(S_{31}) d\xi_1 d\xi_2 \\
& + \int_{\xi_3=\xi_{3\max}} -2\delta p(-S_{31}) d\xi_1 d\xi_2 + \int_{\xi_3=\xi_{3\max}} -2p\delta(-S_{31}) d\xi_1 d\xi_2 - \int_\Omega \frac{\partial \psi^T}{\partial \xi_i} \delta S_{ij} f_j d\Omega \\
& - \int_{\xi_2=0} J\left(\psi_2 \frac{\partial \xi_2}{\partial x_1} + \psi_3 \frac{\partial \xi_2}{\partial x_2} + \psi_4 \frac{\partial \xi_2}{\partial x_3}\right) \delta p d\xi_3 d\xi_1 - \int_{\xi_2=0} \left(\psi_2 \delta S_{21} + \psi_3 \delta S_{22} + \psi_4 \delta S_{23}\right) p d\xi_3 d\xi_1 \\
& + \int_{\xi_2=\xi_{2\max}} J\left(\psi_2 \frac{\partial \xi_2}{\partial x_1} + \psi_3 \frac{\partial \xi_2}{\partial x_2} + \psi_4 \frac{\partial \xi_2}{\partial x_3}\right) \delta p d\xi_3 d\xi_1 + \int_{\xi_2=\xi_{2\max}} \left(\psi_2 \delta S_{21} + \psi_3 \delta S_{22} + \psi_4 \delta S_{23}\right) p d\xi_3 d\xi_1 \\
& - \int_{\xi_3=0} J\left(\psi_2 \frac{\partial \xi_3}{\partial x_1} + \psi_3 \frac{\partial \xi_3}{\partial x_2} + \psi_4 \frac{\partial \xi_3}{\partial x_3}\right) \delta p d\xi_1 d\xi_2 - \int_{\xi_3=0} \left(\psi_2 \delta S_{31} + \psi_3 \delta S_{32} + \psi_4 \delta S_{33}\right) p d\xi_1 d\xi_2 \\
& + \int_{\xi_3=\xi_{3\max}} J\left(\psi_2 \frac{\partial \xi_3}{\partial x_1} + \psi_3 \frac{\partial \xi_3}{\partial x_2} + \psi_4 \frac{\partial \xi_3}{\partial x_3}\right) \delta p d\xi_1 d\xi_2 + \int_{\xi_3=\xi_{3\max}} \left(\psi_2 \delta S_{31} + \psi_3 \delta S_{32} + \psi_4 \delta S_{33}\right) p d\xi_1 d\xi_2
\end{aligned} \tag{B-7}$$

By letting ψ satisfy the following wall boundary conditions

$$\psi_2 S_{21} + \psi_3 S_{22} + \psi_4 S_{23} = -2S_{21} \qquad \text{on} \quad \xi_2 = const \tag{B-8a}$$

$$\psi_2 S_{31} + \psi_3 S_{32} + \psi_4 S_{33} = -2S_{31} \qquad \text{on} \quad \xi_3 = const \tag{B-8b}$$

δp will not appear explicitly in the expression of δI

$$\begin{aligned}
\delta I = & -\int_\Omega \frac{\partial \psi^T}{\partial \xi_i} \delta S_{ij} f_j d\Omega - \int_{\xi_2=0} \left((2+\psi_2)\delta S_{21} + \psi_3 \delta S_{22} + \psi_4 \delta S_{23}\right) p d\xi_3 d\xi_1 \\
& + \int_{\xi_2=\xi_{2\max}} \left((2+\psi_2)\delta S_{21} + \psi_3 \delta S_{22} + \psi_4 \delta S_{23}\right) p d\xi_3 d\xi_1 \\
& - \int_{\xi_3=0} \left((2+\psi_2)\delta S_{31} + \psi_3 \delta S_{32} + \psi_4 \delta S_{33}\right) p d\xi_1 d\xi_2 \\
& + \int_{\xi_3=\xi_{3\max}} \left((2+\psi_2)\delta S_{31} + \psi_3 \delta S_{32} + \psi_4 \delta S_{33}\right) p d\xi_1 d\xi_2
\end{aligned} \tag{B-9}$$

Appendix C. Adjoint Equation in Physical Space and Its Integral Form

The steady-state adjoint equation obtained in Section 4 is

$$C_i^T \frac{\partial \psi}{\partial \xi_i} = 0 \tag{C-1}$$

where

$$C_i = S_{ij} A_j = J K_{ij}^{-1} A_j = J \frac{\partial \xi_i}{\partial x_j} A_j = J \frac{\partial \xi_i}{\partial x_j} \frac{\partial f_j}{\partial w}$$

First, look at the summation terms in Eq. (C-1)

$$C_i^T \frac{\partial \psi}{\partial \xi_i} = \left(J \frac{\partial \xi_i}{\partial x_j} A_j \right)^T \frac{\partial \psi}{\partial \xi_i} = J \frac{\partial \xi_i}{\partial x_j} A_j^T \frac{\partial \psi}{\partial \xi_i} = J \frac{\partial \xi_i}{\partial x_j} A_j^T \left(\frac{\partial \psi}{\partial x_k} \frac{\partial x_k}{\partial \xi_i} \right)$$

$$= J \frac{\partial \xi_i}{\partial x_j} \frac{\partial x_k}{\partial \xi_i} A_j^T \frac{\partial \psi}{\partial x_k} = J \left(\frac{\partial \xi_1}{\partial x_j} \frac{\partial x_k}{\partial \xi_1} + \frac{\partial \xi_2}{\partial x_j} \frac{\partial x_k}{\partial \xi_2} + \frac{\partial \xi_3}{\partial x_j} \frac{\partial x_k}{\partial \xi_3} \right) A_j^T \frac{\partial \psi}{\partial x_k}$$

$$= J \left(\frac{\partial \xi_1}{\partial x_1} \frac{\partial x_k}{\partial \xi_1} + \frac{\partial \xi_2}{\partial x_1} \frac{\partial x_k}{\partial \xi_2} + \frac{\partial \xi_3}{\partial x_1} \frac{\partial x_k}{\partial \xi_3} \right) A_1^T \frac{\partial \psi}{\partial x_k} + J \left(\frac{\partial \xi_1}{\partial x_2} \frac{\partial x_k}{\partial \xi_1} + \frac{\partial \xi_2}{\partial x_2} \frac{\partial x_k}{\partial \xi_2} + \frac{\partial \xi_3}{\partial x_2} \frac{\partial x_k}{\partial \xi_3} \right) A_2^T \frac{\partial \psi}{\partial x_k}$$

$$+ J \left(\frac{\partial \xi_1}{\partial x_3} \frac{\partial x_k}{\partial \xi_1} + \frac{\partial \xi_2}{\partial x_3} \frac{\partial x_k}{\partial \xi_2} + \frac{\partial \xi_3}{\partial x_3} \frac{\partial x_k}{\partial \xi_3} \right) A_3^T \frac{\partial \psi}{\partial x_k} \qquad (sum \quad for \quad j = 1-3)$$

$$= J \left(\frac{\partial \xi_1}{\partial x_1} \frac{\partial x_1}{\partial \xi_1} + \frac{\partial \xi_2}{\partial x_1} \frac{\partial x_1}{\partial \xi_2} + \frac{\partial \xi_3}{\partial x_1} \frac{\partial x_1}{\partial \xi_3} \right) A_1^T \frac{\partial \psi}{\partial x_1} + J \left(\frac{\partial \xi_1}{\partial x_2} \frac{\partial x_1}{\partial \xi_1} + \frac{\partial \xi_2}{\partial x_2} \frac{\partial x_1}{\partial \xi_2} + \frac{\partial \xi_3}{\partial x_2} \frac{\partial x_1}{\partial \xi_3} \right) A_2^T \frac{\partial \psi}{\partial x_1}$$

$$+ J \left(\frac{\partial \xi_1}{\partial x_3} \frac{\partial x_1}{\partial \xi_1} + \frac{\partial \xi_2}{\partial x_3} \frac{\partial x_1}{\partial \xi_2} + \frac{\partial \xi_3}{\partial x_3} \frac{\partial x_1}{\partial \xi_3} \right) A_3^T \frac{\partial \psi}{\partial x_1} (k = 1) + J \left(\frac{\partial \xi_1}{\partial x_1} \frac{\partial x_2}{\partial \xi_1} + \frac{\partial \xi_2}{\partial x_1} \frac{\partial x_2}{\partial \xi_2} + \frac{\partial \xi_3}{\partial x_1} \frac{\partial x_2}{\partial \xi_3} \right) A_1^T \frac{\partial \psi}{\partial x_2}$$

$$+ J \left(\frac{\partial \xi_1}{\partial x_2} \frac{\partial x_2}{\partial \xi_1} + \frac{\partial \xi_2}{\partial x_2} \frac{\partial x_2}{\partial \xi_2} + \frac{\partial \xi_3}{\partial x_2} \frac{\partial x_2}{\partial \xi_3} \right) A_2^T \frac{\partial \psi}{\partial x_2} + J \left(\frac{\partial \xi_1}{\partial x_3} \frac{\partial x_2}{\partial \xi_1} + \frac{\partial \xi_2}{\partial x_3} \frac{\partial x_2}{\partial \xi_2} + \frac{\partial \xi_3}{\partial x_3} \frac{\partial x_2}{\partial \xi_3} \right) A_3^T \frac{\partial \psi}{\partial x_2} (k = 2)$$

$$+ J \left(\frac{\partial \xi_1}{\partial x_1} \frac{\partial x_3}{\partial \xi_1} + \frac{\partial \xi_2}{\partial x_1} \frac{\partial x_3}{\partial \xi_2} + \frac{\partial \xi_3}{\partial x_1} \frac{\partial x_3}{\partial \xi_3} \right) A_1^T \frac{\partial \psi}{\partial x_3} + J \left(\frac{\partial \xi_1}{\partial x_2} \frac{\partial x_3}{\partial \xi_1} + \frac{\partial \xi_2}{\partial x_2} \frac{\partial x_3}{\partial \xi_2} + \frac{\partial \xi_3}{\partial x_2} \frac{\partial x_3}{\partial \xi_3} \right) A_2^T \frac{\partial \psi}{\partial x_3}$$

$$+ J \left(\frac{\partial \xi_1}{\partial x_3} \frac{\partial x_3}{\partial \xi_1} + \frac{\partial \xi_2}{\partial x_3} \frac{\partial x_3}{\partial \xi_2} + \frac{\partial \xi_3}{\partial x_3} \frac{\partial x_3}{\partial \xi_3} \right) A_3^T \frac{\partial \psi}{\partial x_3} (k = 3)$$

Then, notice that for the covariant base vectors and contra-variant base vectors of the curvilinear coordinate system defined as follows, respectively

$$\vec{e}_i = \frac{\partial \vec{r}}{\partial \xi_i}, \quad \vec{e}^{\,i} = \nabla \xi_i \qquad (i = 1,2,3)$$

there exist relations between the two sets of base vectors

$$\vec{e}_i \cdot \vec{e}^{\,j} = \delta_i^{\,j} = \begin{cases} 0, & i \neq j \\ 1, & i = j \end{cases}, \qquad \vec{e}^{\,i} \cdot \vec{e}_j = \delta_j^{\,i} = \begin{cases} 0, & i \neq j \\ 1, & i = j \end{cases} \tag{C-2}$$

The second relation in Eq. (C-2) can be expressed in the following product form of two Jacobian matrices

$$\begin{bmatrix} \frac{\partial \xi_1}{\partial x_1} & \frac{\partial \xi_1}{\partial x_2} & \frac{\partial \xi_1}{\partial x_3} \\ \frac{\partial \xi_2}{\partial x_1} & \frac{\partial \xi_2}{\partial x_2} & \frac{\partial \xi_2}{\partial x_3} \\ \frac{\partial \xi_3}{\partial x_1} & \frac{\partial \xi_3}{\partial x_2} & \frac{\partial \xi_3}{\partial x_3} \end{bmatrix} \begin{bmatrix} \frac{\partial x_1}{\partial \xi_1} & \frac{\partial x_1}{\partial \xi_2} & \frac{\partial x_1}{\partial \xi_3} \\ \frac{\partial x_2}{\partial \xi_1} & \frac{\partial x_2}{\partial \xi_2} & \frac{\partial x_2}{\partial \xi_3} \\ \frac{\partial x_3}{\partial \xi_1} & \frac{\partial x_3}{\partial \xi_2} & \frac{\partial x_3}{\partial \xi_3} \end{bmatrix} = \begin{bmatrix} 1 & 0 & 0 \\ 0 & 1 & 0 \\ 0 & 0 & 1 \end{bmatrix} \tag{C-3}$$

Exchanging the position of the two matrices should lead to the same unit matrix

$$\begin{bmatrix} \frac{\partial x_1}{\partial \xi_1} & \frac{\partial x_1}{\partial \xi_2} & \frac{\partial x_1}{\partial \xi_3} \\ \frac{\partial x_2}{\partial \xi_1} & \frac{\partial x_2}{\partial \xi_2} & \frac{\partial x_2}{\partial \xi_3} \\ \frac{\partial x_3}{\partial \xi_1} & \frac{\partial x_3}{\partial \xi_2} & \frac{\partial x_3}{\partial \xi_3} \end{bmatrix} \begin{bmatrix} \frac{\partial \xi_1}{\partial x_1} & \frac{\partial \xi_1}{\partial x_2} & \frac{\partial \xi_1}{\partial x_3} \\ \frac{\partial \xi_2}{\partial x_1} & \frac{\partial \xi_2}{\partial x_2} & \frac{\partial \xi_2}{\partial x_3} \\ \frac{\partial \xi_3}{\partial x_1} & \frac{\partial \xi_3}{\partial x_2} & \frac{\partial \xi_3}{\partial x_3} \end{bmatrix} = \begin{bmatrix} 1 & 0 & 0 \\ 0 & 1 & 0 \\ 0 & 0 & 1 \end{bmatrix} \tag{C-4}$$

Observing how each element is produced in the unit matrix in Eq. (C-4) will simplify the expression of $C_i^{\,T} \frac{\partial \psi}{\partial \xi_i}$ to the following form

$$C_i^{\,T} \frac{\partial \psi}{\partial \xi_i} = J\left(A_1^T \frac{\partial \psi}{\partial x_1} + A_2^T \frac{\partial \psi}{\partial x_2} + A_3^T \frac{\partial \psi}{\partial x_3} \right) \tag{C-5}$$

Since the Jacobian determinant must not be zero, the steady-state adjoint equation in physical space can be written as

$$A_1^T \frac{\partial \psi}{\partial x_1} + A_2^T \frac{\partial \psi}{\partial x_2} + A_3^T \frac{\partial \psi}{\partial x_3} = 0 \tag{C-6}$$

The time-dependent adjoint equation in physical space can be written as

$$\frac{\partial \psi}{\partial t} - A_1^T \frac{\partial \psi}{\partial x} - A_2^T \frac{\partial \psi}{\partial y} - A_3^T \frac{\partial \psi}{\partial z} = 0 \tag{C-7}$$

From Gauss formula

$$\iiint_V \nabla \cdot \vec{A} dV = \oiint_S \vec{A} \cdot \vec{n} dS$$

let

$$\vec{A} = \psi \vec{i}$$

then

$$\iiint_V \frac{\partial \psi}{\partial x} dV = \oiint_S \psi(\vec{i} \cdot \vec{n}) dS = \oiint_S \psi dS_x \tag{C-8a}$$

Similarly we have

$$\iiint_V \frac{\partial \psi}{\partial y} dV = \oiint_S \psi(\vec{j} \cdot \vec{n}) dS = \oiint_S \psi dS_y \tag{C-8b}$$

$$\iiint_V \frac{\partial \psi}{\partial z} dV = \oiint_S \psi(\vec{k} \cdot \vec{n}) dS = \oiint_S \psi dS_z \tag{C-8c}$$

Now we integrate Eq. (C-7) in a grid cell $V_{i,j,k}$ with A_1^T, A_2^T, A_3^T regarded as constants over the cell

$$\int_{V_{i,j,k}} \frac{\partial \psi}{\partial t} dV - (A_1^T)_{i,j,k} \int_{V_{i,j,k}} \frac{\partial \psi}{\partial x} dV - (A_2^T)_{i,j,k} \int_{V_{i,j,k}} \frac{\partial \psi}{\partial y} dV - (A_3^T)_{i,j,k} \int_{V_{i,j,k}} \frac{\partial \psi}{\partial z} dV = 0 \tag{C-9}$$

Using Gauss formula, we obtain

$$\int_{V_{i,j,k}} \frac{\partial \psi}{\partial t} dV - (A_1^T)_{i,j,k} \oint_{S_{i,j,k}} \psi dS_x - (A_2^T)_{i,j,k} \oint_{S_{i,j,k}} \psi dS_y - (A_3^T)_{i,j,k} \oint_{S_{i,j,k}} \psi dS_z = 0 \tag{C-10}$$

where $S_{i,j,k}$ is the outer face of $V_{i,j,k}$.

Acknowledgments

This work is sponsored by DSTA (Defence Science and Technology Agency) of Singapore under Research Program No. DSTA POD 1820. The first author would like to thank Dr. Liao Yunfei for his great efforts and toil in searching and scanning a lot of literature.

References

[1] Seddon, J., and Goldsmith, E. L., *Intake Aerodynamics*, First published in Great Britain by Collins Professional and Technical Books 1985, Williams Collins Sons & Co. Ltd, 8 Grafton Street, London W1X 3LA.

[2] Weir, L. J., Sanders, B. W., and Vachon, J., "A New Design Concept for Supersonic Axisymmetric Inlets," *38th AIAA/ASME/SAE/ASEE Joint Propulsion Conference & Exhibit*, July 7-10, 2002, Indianapolis, Indiana, USA, AIAA paper 2002-3775.

[3] Gaiddon, A., and Knight, D. D., "Multicriteria Design Optimization of Integrated Three-Dimensional Supersonic Inlets," *Journal of Propulsion and Power*, Vol. 19, No. 3, May-June 2003, pp. 456-463.

[4] Smart, M. K., "Optimization of Two-Dimensional Scramjet Inlets," *Journal of Aircraft*, Vol. 36, No. 2, March-April 1999, pp. 430-433.

[5] Chernyavsky, B., Stepanov, V., Rasheed, K., Blaize, M., and Knight, D., "3-D Hypersonic Inlet Optimization Using a Genetic Algorithm," AIAA paper 98-3582.

[6] Reinartz, B. U., Herrmann, C. D., Ballmann, J., and Koschel, W. W., "Aerodynamic Performance Analysis of a Hypersonic Inlet Isolator Using Computation and Experiment," *Journal of Propulsion and Power*, Vol. 19, No. 5, September-October 2003, pp. 868-875.

[7] Ahsun, U., Merchant, A., Paduano, J. D., and Drela, M., "Design of an Actively Stabilized Near-Isentropic Supersonic Inlet," *16th AIAA Computational Fluid Dynamics Conference*, June 23-26, 2003, Orlando, Florida, USA, AIAA paper 2003-4096.

[8] Fujiwara, H., Murakami, A., and Watanabe, Y., "Numerical Analysis on Shock Oscillation of Two-Dimensional External Compression Intakes," *32nd AIAA Fluid Dynamics Conference*, June 24-26, 2002, St. Louis, Missouri, USA, AIAA paper 2002-2740.

[9] Markopoulos, N., Neumeier, Y., Prasad, J. V. R., and Zinn, B. T., "An Extended Analytical Model for Compressor Rotating Stall and Surge," *35th AIAA/ASME/SAE/ASEE Joint Propulsion Conference & Exhibit*, June 20-24, 1999, Los Angeles, California, USA, AIAA paper 99-2124.

[10] Mayer, D. W., and Paynter, G. C., "Prediction of Supersonic Inlet Unstart Caused by Freestream Disturbances," *AIAA Journal*, Vol. 33, No. 2, February 1995, pp. 266-275.
[11] Rabe, A., Ölçmen, S., Anderson, J., Burdisso, R., Ng, W., "A Facility for Active Flow Control Research in Serpentine Inlets," *40th AIAA Aerospace Sciences Meeting & Exhibit*, January 14-17, 2002, Reno, NV, USA, AIAA paper 2002-0510.
[12] Lefantzi, S., and Knight, D. D., "Automated Design Optimization of a Three-Dimensional S-Shaped Subsonic Diffuser," *Journal of Propulsion and Power*, Vol. 18, No. 4, July-August 2002, pp. 913-921.
[13] Harper, D. K., Leitch, T. A., Ng, W. F., Guillot, S. G., Burdisso, R. A., "Boundary Layer Control and Wall-Pressure Fluctuations in a Serpentine Inlet," *36th AIAA Joint Propulsion Conference*, July 17-19, 2000, Huntsville, Alabama, USA, AIAA paper 2000-3597.
[14] Anderson, B. H., Keller, D., "A Robust Design Methodology for Optimal Micro-Scale Secondary Flow Control in Compact Inlet Diffusers," *40th AIAA Aerospace Sciences Meeting & Exhibit*, January 14-17, 2002, Reno, Nevada, USA, AIAA paper 2002-0541.
[15] Menzies, R. D. D., "Investigation of S-Shaped Intake Aerodynamics Using Computational Fluid Dynamics," Ph. D. Dissertation, Department of Aerospace Engineering, University of Glasgow, United Kingdom, Oct. 2002.
[16] Jameson, A., and Alonso, J. J., "Automatic Aerodynamic Optimization on Distributed Memory Architectures," *34th AIAA Aerospace Sciences Meeting and Exhibit*, January 8-12, 1996, Reno, NV, USA, AIAA paper 96-0409.
[17] Jameson, A., "Optimum Aerodynamic Design Using Control Theory," *Computational Fluid Dynamics Review 1995*, pp. 495-528.
[18] Jameson, A., "Aerodynamic Design Methods," *Solution Techniques for Large-Scale CFD Problems–Computational Methods in Applied Sciences*, 1995, pp. 417-436.
[19] Zhang, Z. K., Lum, K.-Y., "Airfoil Optimization Design of Drag Minimization with Lift Constraint Using Adjoint Equation Method," *44th AIAA Aerospace Sciences Meeting and Exhibit*, Jan. 9-12, 2006, Reno, NV, USA, AIAA paper 2006-55.
[20] Hicks, R. M., and Henne, P. A., "Wing Design by Numerical Optimization," *J. of Aircraft*, Vol. 15, No. 7, July 1978, pp. 407-412.
[21] Eyi, S., Hager, J.O., and Lee, K.D., "Airfoil Design Using the Navier-Stokes Equations," *Journal of Optimization Theory and Applications*, Vol. 83, No. 3, Dec.1994, pp. 447-461.
[22] Jameson, A., "A Perspective on Computational Algorithms for Aerodynamic Analysis and Design," *Sixth Taiwan National Conference on Computational Fluid Dynamics*, Taitung, Taiwan Province, China, Aug. 1999.
[23] Jameson, A., Schmidt, W., and Turkel, E., "Numerical Solution of the Euler Equations by Finite Volume Methods Using Runge-Kutta Time-Stepping Schemes," AIAA paper 81-1259, 1981.
[24] Cai, J. S., "Numerical Analysis of Euler Equations for Transonic Flows at High Angle of Attack," Ph.D. Dissertation, Northwestern Polytechnical University, Xi'an, China, 1992.
[25] Zhang, Z. K., "Multi-grid Numerical Solution of Euler Equations for Transonic Flows around Wing-Body Combination at High Angle of Attack," Ph.D. Dissertation, Northwestern Polytechnical University, Xi'an, China, 1994.
[26] Zhang, Z. K., "Multiblock Grid Generation of Complex Multicomponent Aircraft and Zonal Solutions of Euler Equations for High-Incidence Flows around the Aircraft," Post-Doctoral Research Report, Beijing University of Aeronautics and Astronautics, Beijing, China, 1996.
[27] Wilcox, D. C., *Turbulence Modeling for CFD*, 2nd Ed., DCW Industries, ISBN: 0963605151, 1998. (1st edition, 1993, La Cañada, California)
[28] Kim J., Moin P., Moser R., "Turbulence Statistics in Fully Developed Channel Flow at Low Reynolds Number," *Journal of Fluid Mechanics*, Vol. 177, 1987, pp. 133-166.